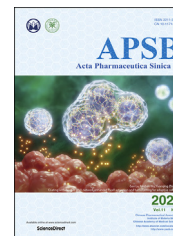




Chinese Pharmaceutical Association
Institute of Materia Medica, Chinese Academy of Medical Sciences

Acta Pharmaceutica Sinica B

www.elsevier.com/locate/apsb
www.sciencedirect.com



ORIGINAL ARTICLE

Polyoxypregnanes as safe, potent, and specific ABCB1-inhibitory pro-drugs to overcome multidrug resistance in cancer chemotherapy *in vitro* and *in vivo*



Xu Wu^{a,b,f,†}, Chun Yin^{a,b,†}, Jiang Ma^{a,b,†}, Stella Chai^{a,b},
Chunyuan Zhang^{a,b}, Sheng Yao^{b,c}, Onat Kadioglu^d, Thomas Efferth^d,
Yang Ye^{b,c}, Kenneth Kin-Wah To^{e,*}, Ge Lin^{a,b,*}

^aSchool of Biomedical Sciences, Faculty of Medicine, the Chinese University of Hong Kong, Hong Kong 999077, China

^bJoint Research Laboratory of Promoting Globalization of Traditional Chinese Medicines between the Chinese University of Hong Kong and Shanghai Institute of Materia Medica, Chinese Academy of Sciences, Hong Kong 999077, China

^cState Key Laboratory of Drug Research and Natural Products Chemistry Department, Shanghai Institute of Materia Medica, Chinese Academy of Sciences, Shanghai 201203, China

^dDepartment of Pharmaceutical Biology, Johannes Gutenberg University, Mainz 55099, Germany

^eSchool of Pharmacy, Faculty of Medicine, the Chinese University of Hong Kong, Hong Kong 999077, China

^fLaboratory of Molecular Pharmacology, Department of Pharmacology, School of Pharmacy, Southwest Medical University, Luzhou 646000, China

Received 18 August 2020; received in revised form 22 October 2020; accepted 29 December 2020

Abbreviations: ABC, ATP-binding cassette; ABCB1, ATP binding cassette subfamily B member 1; ABCC1, ATP binding cassette subfamily C member 1; ABCG2, ATP binding cassette subfamily G member 2; ATF3, activating transcription factor 3; AUC_{0–∞}, area under plasma concentration vs. time curve; BBB, blood–brain barrier; BHI, brain heart infusion; CL, clearance; C_{max}, peak concentration; CYP, cytochrome P450 isozyme; Dox, doxorubicin; ECL, electrochemiluminescence; EVOM, epithelial tissue voltammeter; *F*, bioavailability; FBS, fetal bovine serum; GAPDH, glyceraldehyde-3-phosphate dehydrogenase; HBSS, Hank's balanced salt solution; H&E, hematoxylin and eosin; IC₅₀, half maximal inhibitory concentration; LBE, lowest binding energy; LC–MS, liquid chromatography coupled with mass spectrometry; *M. tenacissima*, *Marsdenia tenacissima*; MDR, multidrug resistance; MDR1a, multidrug resistance protein 1a; MRT, mean residence time; NADPH, reduced nicotinamide adenine dinucleotide phosphate; N.A., not applicable; N.D., not detected; NMPA, National Medical Products Administration; *P*_{app}, apparent permeability; PBS, phosphate buffer saline; PCR, polymerase chain reaction; PE, phycoerythrin; PI, propidium iodide; POP, polyoxypregnane; PXR, pregnane X receptor; qPCR, quantitative PCR; SD, standard derivation; SDS-PAGE, sodium dodecyl sulfate-polyacrylamide gel electrophoresis; *t*_{1/2}, elimination half-life; TEER, transepithelial electrical resistance; *T*_{max}, time for peak concentration; UIC-2, mouse monoclonal ABCB1 antibody; *V*_d, volume of distribution.

*Corresponding authors.

E-mail addresses: kennethto@cuhk.edu.hk (Kenneth Kin-Wah To), linge@cuhk.edu.hk (Ge Lin).

†These authors made equal contributions to this work.

Peer review under responsibility of Chinese Pharmaceutical Association and Institute of Materia Medica, Chinese Academy of Medical Sciences.

<https://doi.org/10.1016/j.apsb.2020.12.021>

2211-3835 © 2021 Chinese Pharmaceutical Association and Institute of Materia Medica, Chinese Academy of Medical Sciences. Production and hosting by Elsevier B.V. This is an open access article under the CC BY-NC-ND license (<http://creativecommons.org/licenses/by-nc-nd/4.0/>).

KEY WORDS

Multidrug resistance;
 ABCB1;
 Polyoxypregnane;
 Combination
 chemotherapy;
Marsdenia tenacissima

Abstract Multidrug resistance (MDR) mediated by ATP binding cassette subfamily B member 1 (ABCB1) is significantly hindering effective cancer chemotherapy. However, currently, no ABCB1-inhibitory drugs have been approved to treat MDR cancer clinically, mainly due to the inhibitor specificity, toxicity, and drug interactions. Here, we reported that three polyoxypregnanes (POPs) as the most abundant constituents of *Marsdenia tenacissima* (*M. tenacissima*) were novel ABCB1-modulatory pro-drugs, which underwent intestinal microbiota-mediated biotransformation *in vivo* to generate active metabolites. The metabolites at non-toxic concentrations restored chemosensitivity in ABCB1-overexpressing cancer cells *via* inhibiting ABCB1 efflux activity without changing ABCB1 protein expression, which were further identified as specific non-competitive inhibitors of ABCB1 showing multiple binding sites within ABCB1 drug cavity. These POPs did not exhibit ABCB1/drug metabolizing enzymes interplay, and their repeated administration generated predictable pharmacokinetic interaction with paclitaxel without obvious toxicity *in vivo*. We further showed that these POPs enhanced the accumulation of paclitaxel in tumors and overcame ABCB1-mediated chemoresistance. The results suggested that these POPs had the potential to be developed as safe, potent, and specific pro-drugs to reverse ABCB1-mediated MDR. Our work also provided scientific evidence for the use of *M. tenacissima* in combinational chemotherapy.

© 2021 Chinese Pharmaceutical Association and Institute of Materia Medica, Chinese Academy of Medical Sciences. Production and hosting by Elsevier B.V. This is an open access article under the CC BY-NC-ND license (<http://creativecommons.org/licenses/by-nc-nd/4.0/>).

1. Introduction

ABCB1 (MDR1/P-gp) is a 170-kDa ATP-dependent membrane transporter belonging to ATP-binding cassette (ABC) transporter family¹. ABCB1 is ubiquitously expressed in liver, kidney, intestine, placenta, adrenal glands, and blood–brain barrier (BBB). Overexpression of ABCB1, which usually results in increased drug efflux, was first recognized as one of the main causes of multidrug resistance (MDR) by Ling and co-workers in 1976^{2,3}. A wide range of cancers, including breast cancers, colon cancers, acute myeloid leukemia, hematological malignancies, and solid tumors, have been associated with ABCB1 overexpression, which confers MDR of many anticancer drugs such as epipodophyllotoxins (etoposide and teniposide), taxanes (paclitaxel and docetaxel), *Vinca* alkaloids (vinblastine and vincristine), and anthracyclines (doxorubicin and daunorubicin). Clinical significance of ABCB1 inhibition as a strategy for MDR reversal has been extensively studied for more than three decades^{4–6}. Many ABCB1 modulators, including some promising third-generation ones (*e.g.*, tariquidar), have been developed^{5,7}. Unfortunately, there are currently no ABCB1-inhibitory drugs being approved to treat MDR cancer clinically, mostly due to the problems associated with specificity, toxicity, and serious drug–drug interactions [including undesirable interplay between transporter and cytochrome P450 enzymes (CYPs), prolonged drug half-life and narrowed drug therapeutic windows]⁸. Recently, a drug repurposing strategy adopted by several research groups emerges as an effective way to identify MDR reversing agents, which attempts to repurpose conventional drugs with known pharmacological and toxicological profiles for overcoming MDR^{9–12}. Similarly, certain natural products, showing a long history of medicinal use and a less-toxic profile, may provide an alternative source to discover novel ideal ABCB1 modulators.

A Chinese medicinal herb, Tong-guan-teng, derived from the dried stems of *Marsdenia tenacissima* (*M. tenacissima*) (Roxb.) Wight et Arn, has a long history of use in traditional Chinese medicine. Its standardized herbal extract which called Xiao-ai-ping has been approved for the treatment of cancers by the

National Medical Products Administration (NMPA) for more than two decades in China^{13–16}. Xiao-ai-ping is well tolerated in patients and frequently used in combination with chemotherapeutic drugs such as paclitaxel receiving good efficacy in prolonging survival of cancer patients^{17–19}. Our previous studies revealed that several constituents, belonging to the chemical class of polyoxypregnanes (POPs), in *M. tenacissima*, were putative reversal agents of MDR in cancer, in particular with ABCB1 inhibitory effect^{20–24}. However, with the unavailability of adequate amounts of these bioactive POPs for further research and development, it remains unclear about the key pharmacologically-relevant determinants of *M. tenacissima*.

In the present study, we demonstrated that three most abundant POPs, *i.e.*, **P1**, **P2**, and **P3** (Fig. 1) in the herbal extract (53%, g/g), were pro-drugs of three respective bioactive POPs, *i.e.*, **P4**, **P5**, and **P6** (Fig. 1), formed *via* intestinal microbiota-mediated biotransformation. Thus, the aim of this study is to explore whether and how the identified pro-drug POPs as safe, potent, and specific ABCB1 inhibitors to reverse MDR in cancer chemotherapy *in vitro* and *in vivo*. This study would provide scientific evidence for the use of a proprietary herbal extract preparation and its major constituents in combination cancer chemotherapy.

2. Materials and methods

2.1. Cells, reagents, and animals

The human intestinal epithelial Caco-2 cell line was obtained from the American Type Culture Collection (Rockville, MD, USA). The human colon cancer cell line SW620 and its doxorubicin-selected ABCB1-overexpressing subline SW620 Ad300²⁵, and human embryonic kidney HEK293 cells stably transfected with pcDNA3.1 vector (HEK293 pcDNA3.1) or wild-type ABCB1 expression vector (HEK293 MDR1)²¹ were generous gifts from Dr. Susan Bates from the National Cancer Institute (Bethesda, MD, USA). Human breast cancer cell lines MDA435/LCC6 and MDA435/LCC6 MDR1²⁶ were kindly provided by Dr. Robert Clarke from Georgetown University (Washington, DC, USA). To

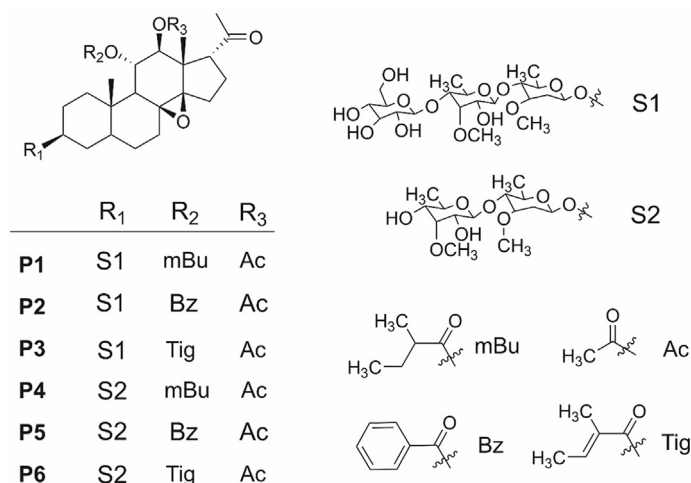


Figure 1 Chemical structures of investigated polyoxypregnanes (POPs). Type I POPs, including **P1** (marsdenoside H), **P2** (marsdenoside K), and **P3** (tenacissoside A), and type II POPs, including **P4** (tenacissoside H), **P5** (tenacissoside I), and **P6** (tenacissoside G), are classified based on the number of sugar moieties in the structures. Ac, acetyl; Bz, benzoyl; mBu, 2-methylbutyryl; Tig, tigloyl.

ensure the correctness of cell models, the expression of ABCB1 in all cell lines was verified and the cytotoxic effect of doxorubicin was compared in paired cell lines (SW620 vs. SW620 Ad300; HEK293 pcDNA3.1 vs. HEK293 MDR1; MDA435/LCC6 vs. MDA435/LCC6 MDR1) (Supporting Information Fig. S1). Cells were grown in RPMI 1640 or DMEM medium supplemented with 10% fetal bovine serum (FBS), 1% penicillin and streptomycin, and were incubated at 37 °C in 5% CO₂. The stable transfected cell lines HEK293 pcDNA3.1 and HEK293 MDR1 were maintained in complete medium supplemented with 2 mg/mL G418.

Monoclonal antibodies against ABCB1 and glyceraldehyde-3-phosphate dehydrogenase (GAPDH) were purchased from Calbiochem (1:1000; C219, San Diego, CA, USA) and Merck Millipore (1:10,000; ABS16, Darmstadt, Germany), respectively. Monoclonal antibody against β -actin (1:2000; 4970) and anti-mouse (1:2000; 7076) or anti-rabbit (1:2000; 7074) IgG horseradish peroxidase conjugate was obtained from Cell Signaling Technology (Boston, MA, USA). Brain heart infusion (BHI) medium was purchased from Becton Dickinson (Franklin Lakes, NJ, USA). Ginsenoside F2 (purity >99%) was purchased from the National Institute for the Control of Pharmaceutical and Biological Products (Beijing, China). Rhodamine 123 (Rh123), doxorubicin, verapamil, sulforhodamine B, paclitaxel, β -glucosidase, heparin, and Tween 80 were obtained from Sigma-Aldrich (MO, USA). PSC833 (valsopodar) was provided by Novartis (East Hanover, NJ, USA). Acetonitrile, methanol, and ethanol were of high performance liquid chromatography (HPLC) grade from RCI Labscan (Bangkok, Thailand). Formic acid was supplied by Merck (Darmstadt, Germany). Distilled water was prepared using a Milli-Q system (Millipore, Bedford, MA, USA). Ketamine and xylazine were obtained from Alfasan (Woerden, Holland). **P1** (marsdenoside H), **P2** (marsdenoside K), **P3** (tenacissoside A), **P4** (tenacissoside H), **P5** (tenacissoside I), and **P6** (tenacissoside G) (purity >98%) were isolated from *M. tenacissima* and characterized by our group as previously reported^{21,22}. Based on the number of sugar moieties in the structure, these POPs are classified into two types, namely type I (**P1**, **P2**, and **P3**) and type II (**P4**, **P5**, and **P6**) POPs (Fig. 1).

Male Sprague-Dawley rats (210–230 g) and male BALB/c nude mice (20–22 g) were supplied by the Laboratory Animal

Service Center, the Chinese University of Hong Kong (Hong Kong, China). Animals were maintained under standard conditions of temperature (22–24 °C), humidity (55%–60%), and a light/dark cycle of 12/12 h, and given food and water ad libitum. A mixed solution containing ketamine (37.5 mg/mL) and xylazine (5 mg/mL) was prepared for anesthetization of animals. The care of animals and all experimental procedures were approved by the Animal Ethics Committee of the Chinese University of Hong Kong.

2.2. Cytotoxicity assay

The anti-proliferative effects of anticancer drugs in MDA435/LCC6 and MDA435/LCC6 MDR1 cells were evaluated by the sulforhodamine B assay as previously described²⁴. The MDR reversal effect of the tested POPs (10 μ mol/L) was assessed by fold changes of the half maximal inhibitory concentration (IC₅₀) value of MDR cells treated with paclitaxel or doxorubicin alone relative to IC₅₀ value of MDR cells treated with combination therapy. PSC833 (0.4 μ mol/L) was used as a positive control.

2.3. Cell cycle and apoptosis assay

The cell cycle and apoptotic assays were conducted by the standard propidium iodide (PI) staining or PI-annexin V co-staining method, respectively, as previously reported^{21,22}. Briefly, the cell cycle distribution and apoptotic cell population were evaluated on MDA435/LCC6 and MDA435/LCC6 MDR1 cells after treatment of paclitaxel alone (20 nmol/L), individual type II POPs (10 μ mol/L), or their combinations for 24 and 48 h, respectively. After staining, an LSRFortessa Cell Analyzer (BD Biosciences, San Jose, CA) was used for flow cytometry analysis.

2.4. Immunoblotting analysis

Cell lysates (30 μ g protein) of SW620 Ad300 cells after treatment of individual POPs at 10 μ mol/L for 72 h were resolved by sodium dodecyl sulfate-polyacrylamide gel electrophoresis (SDS-PAGE) gel and transferred onto a nitrocellulose membrane. After

blocking with 5% nonfat milk, the membranes were probed with anti-ABCB1. β -Actin or GAPDH was applied as loading control. Following incubation with horseradish peroxidase conjugated anti-mouse or anti-rabbit antibodies, protein bands were visualized by chemiluminescence using electrochemiluminescence (ECL) blotting detection reagents.

2.5. Flow cytometry-based substrate efflux assay

The ABCB1 substrate rhodamine 123 (Rh123) efflux assay was performed as previously described⁷. Briefly, MDA435/LCC6 or MDA435/LCC6 MDR1 cells were incubated with Rh123 (0.5 $\mu\text{g}/\text{mL}$) alone or co-incubated with individual POPs at 10 $\mu\text{mol}/\text{L}$, verapamil at 50 $\mu\text{mol}/\text{L}$ and PSC833 at 0.4 $\mu\text{mol}/\text{L}$ (ABCB1 inhibitors as positive controls), respectively, at 37 °C for 30 min. After a 1 h Rh123-free efflux, fluorescence retention in the cells was measured by an LSRFortessa Cell Analyzer.

2.6. Transport study across Caco-2 cell monolayer

Culture of Caco-2 cells and transport of POPs across Caco-2 cell monolayer were performed as previously published²⁷. Briefly, Caco-2 cells were seeded into Transwells (Corning, NY, USA) at 2×10^5 cell/mL for 21–25 days. The integrity was verified by measuring the apparent permeability (P_{app}) values of atenolol and propranolol, a paracellular marker and a transcellular marker, respectively, and the transepithelial electrical resistance (TEER) using an epithelial tissue voltammeter (EVOM) from World Precision Instruments (Sarasota, FL). Monolayers with TEER > 450 $\Omega \cdot \text{cm}^2$ were used for assays. The bidirectional transport (the basolateral to apical (B to A) transport and the apical to basolateral (A to B) transport) assays of individual type II POPs [10 $\mu\text{mol}/\text{L}$ in Hank's balanced salt solution (HBSS)] were performed at 37 °C. At the designated time points, ranging from 15 to 90 min, 400 μL samples were collected from the receiver compartment and 400 μL receiver compartment solution was replaced immediately. Samples were stored at -20 °C until analysis by liquid chromatography coupled with mass spectrometry (LC-MS). P_{app} is calculated as in Eq. (1):

$$P_{\text{app}} = dC/dT \times V/A/C_0 \quad (1)$$

where dC/dT is the initial slope of the plot of cumulative concentrations vs. time ($\mu\text{mol}/\text{L}/\text{s}$); V is the volume of receiver chamber, which is 0.5 mL for the apical side and 1.5 mL for the basolateral side; A is the apparent surface area of the monolayer, which was 1.12 cm^2 for the 12-well transwell plate; C_0 is the initial concentration in donor chamber ($\mu\text{mol}/\text{mL}$).

2.7. ABCB1 ATPase assay

The effect of individual POPs (10 $\mu\text{mol}/\text{L}$) on ATPase activity of human recombinant ABCB1 in a cell membrane fraction was measured by Pgp-Glo™ Assay Systems (V3601, Promega) according to the manufacturer's instruction. Verapamil (an ABCB1 ATPase stimulator) at 50 $\mu\text{mol}/\text{L}$ and PSC833 (an ABCB1 ATPase inhibitor) at 0.4 $\mu\text{mol}/\text{L}$ were used as the positive controls.

2.8. Mouse monoclonal ABCB1 antibody (UIC-2) shift assay

The binding of the conformation sensitive anti-ABCB1 UIC-2 antibody to the transporter protein ABCB1 in MDA435/LCC6

MDR1 cells was measured by flow cytometer as previously described²⁸. Briefly, cells were incubated with individual POPs (1, 5, or 10 $\mu\text{mol}/\text{L}$) in 2% FBS at 37 °C in 5% CO_2 for 10 min before labeled with 0.5 $\mu\text{g}/\text{mL}$ phycoerythrin (PE)-conjugated UIC-2 antibody or IgG2b negative control antibody for another 45 min. Cells were then washed twice with cold phosphate buffer saline (PBS) and stored on ice before the analysis by an LSRFortessa Cell Analyzer. Oxaliplatin, which is not an ABCB1 substrate or inhibitor, was used as a negative control. Verapamil (50 $\mu\text{mol}/\text{L}$) and PSC833 (0.4 $\mu\text{mol}/\text{L}$) were used as positive controls.

2.9. Molecular docking

Docking calculations were performed on AutoDock 4.2 (the Scripps Research Institute, La Jolla, CA, USA) using the human ABCB1 homology model as previously described^{24,29}. Both inactive and active conformations of ABCB1 were used for docking analysis. For co-docking calculations, verapamil and PSC833 were pre-docked on ABCB1 and their effects on the lowest binding energies (LBEs) and interacting residues of individual POPs were evaluated. Because all compounds mainly docked to the drug binding pocket, we focused on this site for the co-docking calculations.

2.10. Pharmacokinetics study of POPs

A type I POPs mixture containing **P1**, **P2**, and **P3** was prepared at the weight composition of 1.4:1:1.1, which was equivalent to their composition in the original herb²³. Vehicle A (Tween 80/saline, 5%/95%) was used to prepare type I POPs mixture solution. Right jugular cannulation was performed on rats for drug administration and blood sampling on the day before the treatment. Rats were randomly divided into three groups (6/group). The rats in group 1 or 2 received intravenously (5 mg/kg) or orally (50 mg/kg) type I POPs mixture. The rats in group 3 received orally antibiotics (containing 200 mg/kg neomycin sulfate, 200 mg/kg streptomycin sulfate, and 200 mg/kg bacitracin) every 12 h (twice daily) for 5 consecutive days and then orally 50 mg/kg type I POPs mixture at 4 h after the last treatment of antibiotics. After type I POPs mixture treatment, 0.2 mL of blood were collected from the catheter at 2, 5, 15, 30, and 45 min, and 1, 2, 4, 8, 9, 12, and 24 h into heparinized tube. After each blood sampling, rats immediately received an equal volume of isotonic saline to composite the blood loss. The collected blood samples were then centrifuged at 6000 $\times g$ for 10 min to obtain plasma and stored at -20 °C until LC-MS analysis.

2.11. Incubation with intestinal microbiota or β -glucosidase

Intestinal microbiota extracted from pooled human fecal samples was used to investigate the hydrolysis of type I POPs. Fresh human fecal samples were collected from four healthy Chinese volunteers (two male and two female, aged 20–32). The microbiota solution was prepared as described previously²⁷. To assure maximum viability of microbiota, the anaerobic bacteria, during the experiment, individual POPs (50 $\mu\text{mol}/\text{L}$) was incubated anaerobically in the Anaerobe Pouch System (GasPak™ EZ, BD Biosciences) containing 25 μL of microbiota solution in BHI medium at 37 °C for 0, 0.5, 1, 2, 3, 6, 9, 12, and 24 h. Reactions were stopped by the addition of an equal volume of ice-cold methanol, followed by immediate centrifugation at 15,000 $\times g$ for

10 min. Supernatant was collected for LC–MS analysis. The percentage of parent POP metabolized (metabolic rate) and metabolite formed (metabolite formation rate) were calculated in Eqs. (2) and (3), respectively:

Metabolic rate

$$= C_t (\text{parent POP, } \mu\text{mol/L}) / C_0 (\text{parent POP, } \mu\text{mol/L}) \times 100\% \quad (2)$$

Metabolite formation rate

$$= C_t (\text{metabolite, } \mu\text{mol/L}) / C_0 (\text{parent POP, } \mu\text{mol/L}) \times 100\% \quad (3)$$

where C_t represents the concentration at designated time points and C_0 represents the concentration of parent POP at time zero.

β -Glucosidases, which hydrolyze β -glucopyranoside linkage from the non-reducing end of β -glucosides, are one of the most abundant enzymes distributed in animals, plants and microorganisms. To investigate whether β -glucosidase is responsible for the hydrolysis of type I POPs into type II POPs, the hydrolysis reaction was performed in a 100 mmol/L phosphate buffer (200 μ L, pH 7.0) containing 800 ng/mL β -glucosidase and individual type I POPs (10 μ mol/L) at 37 °C for 2 h. Then, 200 μ L ice-cold methanol containing 500 nmol/L ginsenoside F2 (internal standard) were added into the mixture for stopping the reaction. Samples were vortexed for 1 min and centrifuged for 15 min at 15,000 \times g, and supernatants were filtered and collected for LC–MS analysis.

2.12. Pharmacokinetic study of paclitaxel

Rats were randomly divided into six groups (6/group) receiving 50 mg/kg of type I POPs orally and 6 mg/kg of paclitaxel intravenously. Vehicle B (ethanol/Tween 80/saline, 5%/5%/90%) was used to prepare paclitaxel solution. Dosage regimen and sampling procedures were: group 1 or 2, vehicle A or type I POPs was administered 8 h prior to paclitaxel; group 3 or 4, vehicle A or type I POPs was administered once-daily for 7 consecutive days. On Day 7, paclitaxel was given at 8 h after type I POPs. For groups 1–4, blood (0.2 mL/sample) was collected as aforementioned with saline compensation at 0, 2, 5, 15, and 30 min, and 1, 2, 4, 6, 8, 10, 12, and 24 h, and feces and urine were collected within 0–24 h after paclitaxel dosing; group 5 or 6, vehicle A or type I POPs was given 8 h prior to paclitaxel once-daily for 6 consecutive days. On Day 1, five blood samples were collected at 5 min prior to type I POPs dosing, 5 min prior to paclitaxel dosing, and 2 min, 1 h, and 8 h after paclitaxel dosing. During Days 2–6, three blood samples were collected at 5 min prior to type I POPs dosing, 5 min prior to paclitaxel dosing and 2 min after paclitaxel dosing. On Day 6, pharmacokinetics of paclitaxel was monitored by measuring blood samples collected at 2, 15, and 30 min, and 1, 3, 6, 8, and 24 h after its last-dose. Tissue (heart, liver, spleen, lung, kidney, and brain) specimens were collected at the end of experiments. The collected blood samples were centrifuged at 6000 \times g for 10 min to obtain plasma, feces, and urine samples were weighed, and tissue specimens were washed with cold PBS, blotted dry, and weighed. All these samples were stored at –80 °C until LC–MS analysis.

2.13. Cocktail assay

Pooled rat liver microsomes from six rats were prepared following the published report³⁰. The cocktail assay has been described previously³⁰. Substrates of individual cytochrome P450 isozymes (CYPs) and their final concentrations for the incubations were: nifedipine (10 μ mol/L, rat CYP3A1/2 substrate), *S*-mephenytoin (20 μ mol/L, rat CYP2C11 substrate), coumarin (2 μ mol/L, rat CYP2A2 substrate), bupropion (5 μ mol/L, rat CYP2B1 substrate), dextromethorphan (20 μ mol/L, rat CYP2D1 substrate), and phenacetin (20 μ mol/L, rat CYP1A2 substrate). A reaction mixture (200 μ L) containing microsomes and substrates with or without individual POPs (10 μ mol/L) was pre-incubated for 5 min at 37 °C in a shaking incubator block before the addition of reduced nicotinamide adenine dinucleotide phosphate (NADPH) regeneration system to initiate the reaction. Each reaction was stopped after 60 min by the addition of 200 μ L of ice-cold methanol containing 500 nmol/L ginsenoside F2 (internal standard). Samples were vortexed for 1 min and centrifuged for 15 min at 15,000 \times g, and supernatants were filtered and collected for LC–MS analysis.

2.14. Toxicity study and total CYPs content measurement

Four rats were treated orally with vehicle or type I POPs (50 mg/kg/day) for 7 consecutive days with daily measurement of body weight. Rats were sacrificed at Day 8. Liver, kidney, lung, heart, spleen, and small intestine (duodenum) were collected, rinsed with cold PBS, blotted dry, and stored for analysis. Histological studies of the collected tissue specimens were conducted by hematoxylin and eosin (H&E) staining following our previous report³¹. The total CYPs content in liver microsomes prepared from type I POPs-treated or untreated rats was determined using reduced CO-difference spectra as previously described³².

2.15. Real-time reverse transcription-polymerase chain reaction (PCR)

Total RNA isolation from rat liver, small intestine (duodenum), and kidney was performed using Trizol reagent (Ambion, Life Technologies) following the manufacturer's protocol. Reverse transcription PCR was carried out using PrimeScript RT reagent kit (TaKaRa). Quantitative PCR (qPCR) analysis was performed in an ABI ViiA 7 Real Time PCR System (Applied Biosystem, Thermo Fisher Scientific) using SYBR Green Real Time PCR kit (Applied Biosystems, life technologies). Primers of *Gapdh*, multi-drug resistance-1a (*Mdr1a*), *Cyp3a1*, *Cyp2c11*, *Cyp1a2*, *Cyp2a2*, *Cyp2b2*, and *Cyp2d1* for quantitative PCR (qPCR) reactions are shown in Supporting Information Table S1.

2.16. Tumor xenograft mouse model

Drug treatments were evaluated in the parental sensitive MDA435/LCC6 and ABCB1-overexpressing resistant MDA435/LCC6 MDR1 xenograft models. MDA435/LCC6 or MDA435/LCC6 MDR1 cells (1×10^6 cells per mouse) were subcutaneously inoculated into the left flank of BALB/c nude mice. When a palpable tumor appeared (approximately 400 mm³), tumor-bearing mice were randomly allocated into 4 groups (5/group). Mice were treated on every other day for 10 days as follows: group 1 or

Table 1 Pharmacokinetic parameters of **P1**, **P2**, and **P3**, and their respective metabolites of **P4**, **P5**, and **P6** after an intravenous or oral administration of type I POPs in rats.

Parameter	Type I POP (iv, 5 mg/kg)			Type I POP (po, 50 mg/kg)					
	P1	P2	P3	P1	P2	P3	P4	P5	P6
T_{max} (h)	N.A.	N.A.	N.A.	0.25 ± 0.00	0.56 ± 0.16	0.31 ± 0.06	8.50 ± 0.50	8.75 ± 0.48	7.50 ± 0.96
C_{max} (mg/L)	N.A.	N.A.	N.A.	0.17 ± 0.02	0.04 ± 0.00	0.11 ± 0.02	1.19 ± 0.09	0.91 ± 0.10	1.14 ± 0.07
$AUC_{0-\infty}$ (mg·h/L)	1.80 ± 0.432	4.04 ± 0.327	2.76 ± 0.193	0.80 ± 0.17	0.27 ± 0.04	0.40 ± 0.07	7.44 ± 0.42	4.84 ± 0.30	6.35 ± 0.40
$t_{1/2}$ (h)	0.119 ± 0.016	0.169 ± 0.003	0.286 ± 0.016	4.17 ± 0.77	6.55 ± 1.88	2.99 ± 0.37	2.54 ± 0.04	2.15 ± 0.23	2.38 ± 0.15
$MRT_{0-\infty}$ (h)	0.190 ± 0.026	0.225 ± 0.005	0.393 ± 0.026	5.12 ± 0.51	6.30 ± 1.36	4.19 ± 0.28	8.62 ± 0.37	9.27 ± 0.42	8.13 ± 0.47
V_d/F (L/kg)	0.103 ± 0.014	0.061 ± 0.005	0.153 ± 0.019	5.14 ± 0.31	3.33 ± 0.51	2.41 ± 0.21	N.A.	N.A.	N.A.
CL/F (L/h/kg)	0.640 ± 0.112	0.253 ± 0.020	0.367 ± 0.026	0.97 ± 0.21	0.40 ± 0.06	0.59 ± 0.09	N.A.	N.A.	N.A.
F (%)	N.A.	N.A.	N.A.	4.45	0.678	1.45	N.A.	N.A.	N.A.

N.A.: Not applicable. Data are expressed as mean ± SD ($n = 6$). T_{max} , time for peak concentration; C_{max} , peak concentration; $AUC_{0-\infty}$, area under plasma concentration vs. time curve; $t_{1/2}$, elimination half-life; MRT, mean residence time; V_d , volume of distribution; CL, clearance; F , bioavailability.

2, animals received vehicle A orally at 2 h prior to intravenous injection of vehicle B or 12 mg/kg paclitaxel; group 3 or 4, animals received 200 mg/kg type I POPs orally at 2 h prior to vehicle B or paclitaxel. The tumor sizes were measured with vernier calipers and tumor volumes were calculated by the formula [(shortest diameter)² × (longest diameter)]/2. All mice were euthanized on Day 11, and tumors and other tissues were excised and stored at -80°C .

2.17. LC–MS analysis

Sample preparation and LC–MS methods developed for quantification are described in Supporting Information.

2.18. Data and statistical analysis

Non-compartmental method using WinNonlin version 4.0 (Pharsight, Mountain View, CA, USA) was applied for pharmacokinetic parameters calculation. Statistical analysis was applied using unpaired two-tailed Student's t -test for comparison between two groups, or one-way or two-way ANOVA with a *post hoc* Tukey test for comparison among three or more groups. A P value less than 0.05 was considered as significant. All data are presented as mean values ± standard derivation (SD).

3. Results

3.1. Type I POPs are biotransformed into type II POPs by intestinal microbiota

After oral administration, type I POPs (**P1**, **P2**, and **P3**) had very low bioavailability (0.68%–4.45%, Table 1) due to their dramatically biotransformed into type II POPs (**P4**, **P5**, and **P6**). The converted type II POPs peaked at about 8 h displayed high systemic exposures (Fig. 2A) with C_{max} values ranging from 0.91 ± 0.1 to 1.19 ± 0.09 mg/L and $AUC_{0-\infty}$ values from 4.84 ± 0.30 to 7.44 ± 0.42 mg·h/L, while type I POPs showed much less systemic exposure with C_{max} values from 0.04 ± 0.00 to 0.17 ± 0.02 mg/L and $AUC_{0-\infty}$ values from 0.27 ± 0.04 to 0.80 ± 0.17 mg·h/L (Table 1). However, these biotransformations were almost negligible in the antibiotics-pretreated rats with only trace amounts of **P4**, **P5**, and **P6** detected in the plasma (Fig. 2B). Further intestinal microbiota incubation demonstrated that **P1**, **P2**,

and **P3** were completely converted into **P4**, **P5**, and **P6**, respectively, within ~ 8 h (Fig. 2C–E), while liver microsomal incubation did not mediate the same conversion (Supporting Information Fig. S2). All the results suggest that intestinal microbiota played an important role in biotransformation of type I to type II POPs. Further study confirm that β -glucosidase, a common enzyme in intestinal bacteria, was responsible for the conversion (Fig. 2F–H). In summary, type I POPs are biotransformed into the respective type II POPs via hydrolysis of the terminal glucose in type I POPs primarily mediated by β -glucosidase in intestinal microbiota.

3.2. Type II but not type I POPs sensitize ABCB1-overexpressing cancer cells to ABCB1 substrate chemotherapeutics

Type II POPs, *i.e.*, **P4**, **P5**, and **P6**, were identified as ABCB1 inhibitors in our previous study using the drug-selected ABCB1-overexpressing SW620 Ad300 cells²⁴. As MDR of chemotherapeutics is mediated by multiple mechanisms³³, in the present study, MDA435/LCC6 and ABCB1-transfected MDA435/LCC6 MDR1 cells were used for studying the role of ABCB1 in MDR (Fig. 3). In order to determine the concentration of POPs for the MDR reversal study, we firstly evaluated the effect of different concentrations of all tested POPs to the cells. The concentration of 10 $\mu\text{mol/L}$ was selected because all the tested POPs did not appreciably affect cell viability at or below 10 $\mu\text{mol/L}$. The results demonstrated that all type II POPs, but not type I POPs at 10 $\mu\text{mol/L}$ significantly inhibited ABCB1-mediated MDR of paclitaxel and doxorubicin (both are ABCB1 substrates) in MDA435/LCC6 MDR1 cells (Table 2 and Fig. 3A–F). Strikingly, the reversal effect of type II POPs was 4.4–4.6 times superior (**P4** and **P5**) or at least comparable (**P6**) to that of verapamil (Table 2). Overall, type II POPs potently sensitize ABCB1 substrate anticancer agents to ABCB1-overexpressing MDR cells.

To further confirm the mechanism underlying circumvention of ABCB1-mediated MDR caused by type II POPs was mainly due to the inhibition of ABCB1 activity, we performed cell cycle and apoptosis studies. In MDA435/LCC6 cells, the results show that paclitaxel induced a significant G2/M phase cell cycle arrest (Fig. 3G) and apoptosis (Fig. 3I), and such effects were not enhanced by the combination treatment with type II POPs. In the resistant MDA435/LCC6 MDR1 cells, paclitaxel alone did not

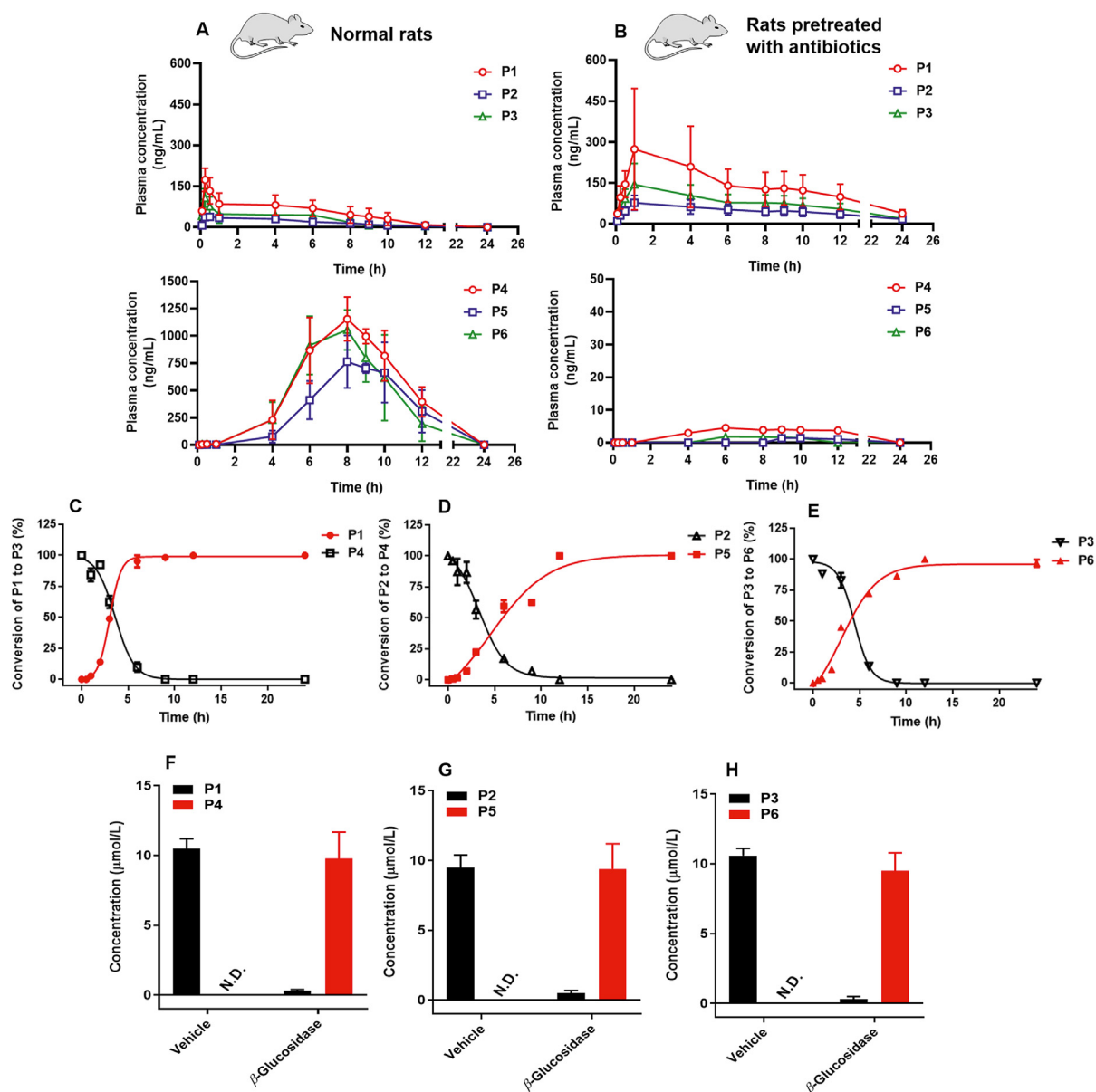


Figure 2 Gut microbiota-mediated biotransformation of type I POPs to type II POPs. The plasma concentration vs. time curve of **P1**, **P2**, and **P3** and their respective metabolites **P4**, **P5**, and **P6** after an oral administration of 50 mg/kg type I POPs mixture to normal rats (A), or to rats orally pretreated with antibiotics for 5 days (B). Conversion of **P1**, **P2**, or **P3** to their respective metabolites in the incubation with intestinal microbiota within 24 h (C)–(E), or with β -glucosidase for 2 h (F)–(H). Black and red curves in (C)–(E) represent metabolic rate and metabolite formation rate, respectively. N.D., not detected. All data are expressed as mean \pm standard deviation (SD) ($n = 6$ for pharmacokinetic study; $n = 4$ for *in vitro* incubation study).

induce G2/M phase cell cycle arrest and apoptosis, while the addition of Type II POPs completely (**P4** or **P5**) or partially (**P6**) restored G2/M phase cell cycle arrest (Fig. 3H) and apoptosis (Fig. 3J) induced by paclitaxel. On the other hand, both type I and type II POPs themselves have no effect on cell cycle and did not cause apoptosis in both parental and ABCB1-mediated MDR cancer cells (Fig. 3H–J). The results imply that type II but not type I POPs sensitize paclitaxel to MDA435/LCC6 MDR1 cells through restoration of paclitaxel-induced cell cycle arrest and apoptosis. Notably, type I POPs are biotransformed to type II POPs in the body, and thus identified as ABCB1-modulatory prodrugs.

3.3. Type II POPs inhibit the efflux activity of ABCB1 via interaction and induction of ABCB1 conformational change

Type II but not type I POPs dose-dependently inhibited ABCB1-mediated Rh123 efflux in MDA435/LCC6MDR1 cells (Fig. 4A) but not in MDA435/LCC6 cells (Fig. 4B), indicating that the efflux inhibition was specific. The efflux inhibition of type II POPs was superior (**P4** and **P5**) or comparable (**P6**) to that of verapamil (Fig. 4A, right panel), further confirming that type II POPs suppress ABCB1-mediated efflux activity. On the other hand, the results from permeability study in Caco-2 monolayer model showed that the ratio of $P_{app(B \rightarrow A)}$ to $P_{app(A \rightarrow B)}$ of all

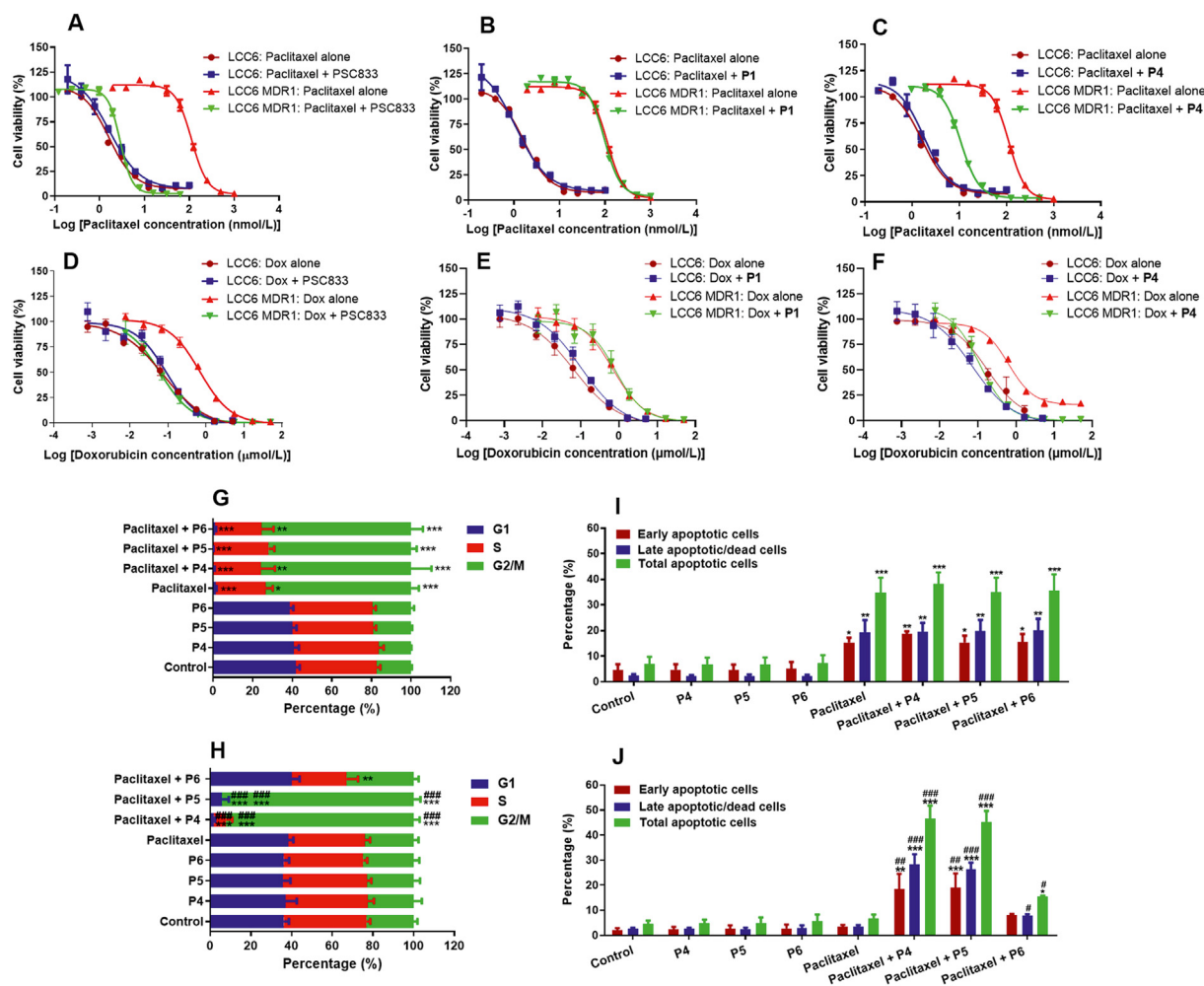


Figure 3 Type II POPs but not type I POPs overcome ATP binding cassette subfamily B member 1 (ABCB1)-mediated multidrug resistance (MDR) of paclitaxel and doxorubicin in MDA435/LCC6 MDR1 cells. Cytotoxicity of paclitaxel (A)–(C) and doxorubicin (Dox) (D)–(F) in MDA435/LCC6 and ABCB1-transfected MDA435/LCC6 MDR1 cells in the absence or presence of PSC833, **P1**, or **P4**. Effect of type II POPs (**P4**, **P5**, or **P6**) on paclitaxel-induced cell cycle arrest in MDA435/LCC6 (G) and MDA435/LCC6 MDR1 (H) cells, and on paclitaxel-induced apoptosis in MDA435/LCC6 (I) and MDA435/LCC6 MDR1 (J) cells. All data are expressed as mean \pm SD ($n = 3$). * $P < 0.05$, ** $P < 0.01$, *** $P < 0.001$, compared to the corresponding subgroups in control group; # $P < 0.05$, ## $P < 0.01$, ### $P < 0.001$, compared to the corresponding subgroups in paclitaxel alone group, by two-way ANOVA test followed by Tukey *post hoc* test.

type II POPs ranged from 1.010 to 1.429, indicating that these POPs were not actively transported from the basolateral to apical sides (Table 3), demonstrating that type II POPs are not ABCB1 substrates and thus not competitive inhibitors of ABCB1.

The mechanistic study was further conducted. Firstly, neither type II POPs (**P4**, **P5**, or **P6**) nor type I POPs (represented by **P1**) appreciably changed the protein expression level of ABCB1 in SW620 Ad300 cells (Fig. 4C), demonstrating that type II POPs inhibit ABCB1 transport function without altering its expression. Secondly, type II but not type I POPs significantly stimulated ABCB1 ATPase activity in a way similar to the competitive inhibitor verapamil (Fig. 4D). It has been reported that ATPase activity of ABCB1 is activated when the substrates are transported by ABCB1 or certain conformational changes occur in ABCB1, such as cross-linking of N-terminal and central regions of ABCB1 nucleotide-binding domains³⁴. Apparently as non-ABCB1 substrates, type II POPs might possibly induce conformational change of ABCB1 *via* interaction with rather than competitive transportation by ABCB1. Therefore, thirdly, UIC-2 shift assay, in

which a conformation sensitive monoclonal antibody UIC-2 binds to an extracellular loop of ABCB1 and the binding of UIC-2 to ABCB1 is increased in certain conformations of ABCB1, especially in the presence of substrates/modulators or ATP hydrolyzing agents²⁶, was further performed. The results reveal that in the presence of type II but not type I POPs, the interaction between UIC-2 and ABCB1 was significantly enhanced in a concentration-dependent manner (Fig. 4E), suggesting that type II POPs interacted with ABCB1 and changed its conformation.

All above data indicate that type II POPs stimulated ABCB1 ATPase activity *via* altering the conformation of ABCB1 but not being transported by ABCB1, in a way similar to tariquidar (a known ABCB1 inhibitor) but different from verapamil (an ABCB1 substrate stimulating ATPase activity) and PSC833 (a non-ABCB1 substrate inhibiting ATPase activity)¹². To further test this hypothesis, we performed interaction analysis of type II POPs with ABCB1 (in both inactive and active conformations) using *in silico* molecular docking. Our previous report indicated that **P4**, **P5**, and **P6** predominantly docked to the drug binding

Table 2 Reversal effect of type II POPs (**P4**, **P5**, and **P6**) on ABCB1-mediated paclitaxel or doxorubicin MDR in MDA435/LCC6 MDR1 resistant cells.

Drug treatment	IC ₅₀ of paclitaxel or doxorubicin (nmol/L)		
	MDA435/LCC6	MDA435/LCC6 MDR1	Fold change ^a
Paclitaxel alone	1.36 ± 0.14	119.50 ± 9.44	N.A.
+PSC833 (0.4 μmol/L)	1.39 ± 0.16	2.01 ± 0.45***	59
+Verapamil (10 μmol/L)	1.29 ± 0.13	25.1 ± 4.45***	5
+ P4 (10 μmol/L)	1.41 ± 0.20	5.33 ± 2.52***	22
+ P5 (10 μmol/L)	1.29 ± 0.12	5.23 ± 2.51***	23
+ P6 (10 μmol/L)	1.26 ± 0.04	32.46 ± 2.16***	4
+ P1 (10 μmol/L)	1.19 ± 0.05	105.18 ± 7.45	1
+ P2 (10 μmol/L)	1.14 ± 0.15	101.09 ± 3.55	1
+ P3 (10 μmol/L)	1.20 ± 0.09	98.58 ± 8.41	1
Doxorubicin alone	76 ± 8	695 ± 40	N.A.
+PSC833 (0.4 μmol/L)	95 ± 6	62 ± 6***	11
+Verapamil (10 μmol/L)	80 ± 9	175 ± 31***	4
+ P4 (10 μmol/L)	72 ± 7	111 ± 10***	6
+ P5 (10 μmol/L)	55 ± 7	50 ± 9***	14
+ P6 (10 μmol/L)	86 ± 6	192 ± 7***	4
+ P1 (10 μmol/L)	90 ± 6	725 ± 61	1
+ P2 (10 μmol/L)	93 ± 7	791 ± 35	1
+ P3 (10 μmol/L)	92 ± 9	755 ± 33	1

+: combination with paclitaxel or doxorubicin. Except for fold change, data are expressed as mean ± SD ($n = 3$). *** $P < 0.001$, compared to the IC₅₀ value of paclitaxel or doxorubicin alone in MDA435/LCC6 MDR1 cells.

^aFold change = IC₅₀ of paclitaxel or doxorubicin alone in MDA435/LCC6 MDR1 cells/IC₅₀ of paclitaxel or doxorubicin in combination with the indicated compounds.

pocket of the inactive conformation of ABCB1 and well fitted into the drug cavity²⁴. Further docking with inactive ABCB1 conformation pre-docked with verapamil or PSC833 showed that **P4**, **P5**, or **P6** in the co-docking analysis revealed significantly lower LBE values, and that the interacting amino acid residues were quite different from the single docking (Supporting Information Table S2). These data indicate that **P4**, **P5**, and **P6** displayed alternative binding sites within the drug-binding pocket of ABCB1. In order to further evaluate that **P4**, **P5**, and **P6** present an interacting mode with ABCB1 similar to tariquidar, docking analysis on inactive and active conformations of ABCB1 was conducted. As shown in Fig. 4F and Table 4, **P4**, **P5**, and **P6** were strongly bound to the inactive ABCB1 conformation in the range of -8 kcal/mol and the docking poses were similar with that of tariquidar. Notably, **P5** was bound in close proximity to tariquidar for both inactive and active ABCB1 conformations, implying the similar activity of **P5** with tariquidar. Moreover, **P5** revealed stronger interaction than **P4** and **P6** with active ABCB1 conformation. The overall results demonstrate that **P4**, **P5**, and **P6** (especially **P5**) interact with both inactive and active conformations of ABCB1 and have a similar binding mode and effect like tariquidar.

3.4. Type I POPs as ABCB1 modulatory pro-drugs induce predictable pharmacokinetic interaction with paclitaxel in rats

Subsequently, we systemically evaluated the potential pharmacokinetic interaction between the ABCB1-modulating POPs with paclitaxel *in vivo*. Type I POPs mixture, as the three most abundant POPs in *M. tenacissima* and putative pro-drugs of type II POPs, were orally administered to animals for the pharmacokinetic interaction study (Fig. 5). A single oral dose of type I POPs mixture dramatically increased the plasma concentrations of paclitaxel in rats (Fig. 5A). AUC_{0–24 h} of paclitaxel was significantly elevated to 62%, while $t_{1/2}$, C_{max} , and mean residence time (MRT_{0–∞}) of

paclitaxel were not changed ($P > 0.05$) by type I POPs (Table 5). Notably, the repeated administration of type I POPs mixture for 7 days exerted a similar effect on paclitaxel pharmacokinetics with 64% increase in AUC_{0–24 h} but unchanged $t_{1/2}$, C_{max} , and MRT_{0–24 h} (Fig. 5E and Table 5). Excretion study showed that the increased systemic exposure of paclitaxel was mainly due to its remarkably inhibited fecal/biliary excretion that was presumably mediated by ABCB1 (Fig. 5B and F, and Supporting Information Fig. S3). The results also demonstrate that type I POPs mixture (1) did not significantly alter tissue distribution profile (Fig. 5C) and metabolism (Fig. 5D) of paclitaxel; (2) did not affect the activities of major drug metabolizing enzymes, including CYP3A1, 2C11, 2A1, 2D1, and 1A2 (Table 6); and (3) did not alter the expression of ABCB1 (Fig. 6A and B) and major CYPs (Fig. 6C) in the body, and total content of CYPs in the liver (Fig. 6D) after 7 days repeated treatment. The findings of type I POPs mixture-induced controllable pharmacokinetic interaction with the increased systemic exposure but unchanged other pharmacokinetic parameters of paclitaxel are beneficial for future designing dosage regimen of paclitaxel combination therapy with type I POPs mixture.

Furthermore, the effect of type I POPs mixture on pharmacokinetics of repeated doses of paclitaxel was evaluated (Fig. 7). In rats daily receiving paclitaxel alone or with type I POPs mixture for 6 consecutive days, again significantly increased systemic exposure (plasma AUC_{0–24 h}) of paclitaxel was observed daily in the combination treatment (Fig. 7A and C), while there were no significant differences in peak and trough plasma concentration (C_{max} and C_{trough}) of paclitaxel after the last dose in paclitaxel alone group (2976 ± 299 and 15.8 ± 6.6 nmol/L) and combination treatment group (3252 ± 397 and 24.0 ± 5.2 nmol/L) (Fig. 7A). The daily paclitaxel accumulation (indicated by the ratio of plasma AUC_{0–24 h, last-dose}/AUC_{0–24 h, first-dose}) was no significant difference between both treated groups (Fig. 7B), and the elimination $t_{1/2}$ of paclitaxel was not changed (paclitaxel group vs.

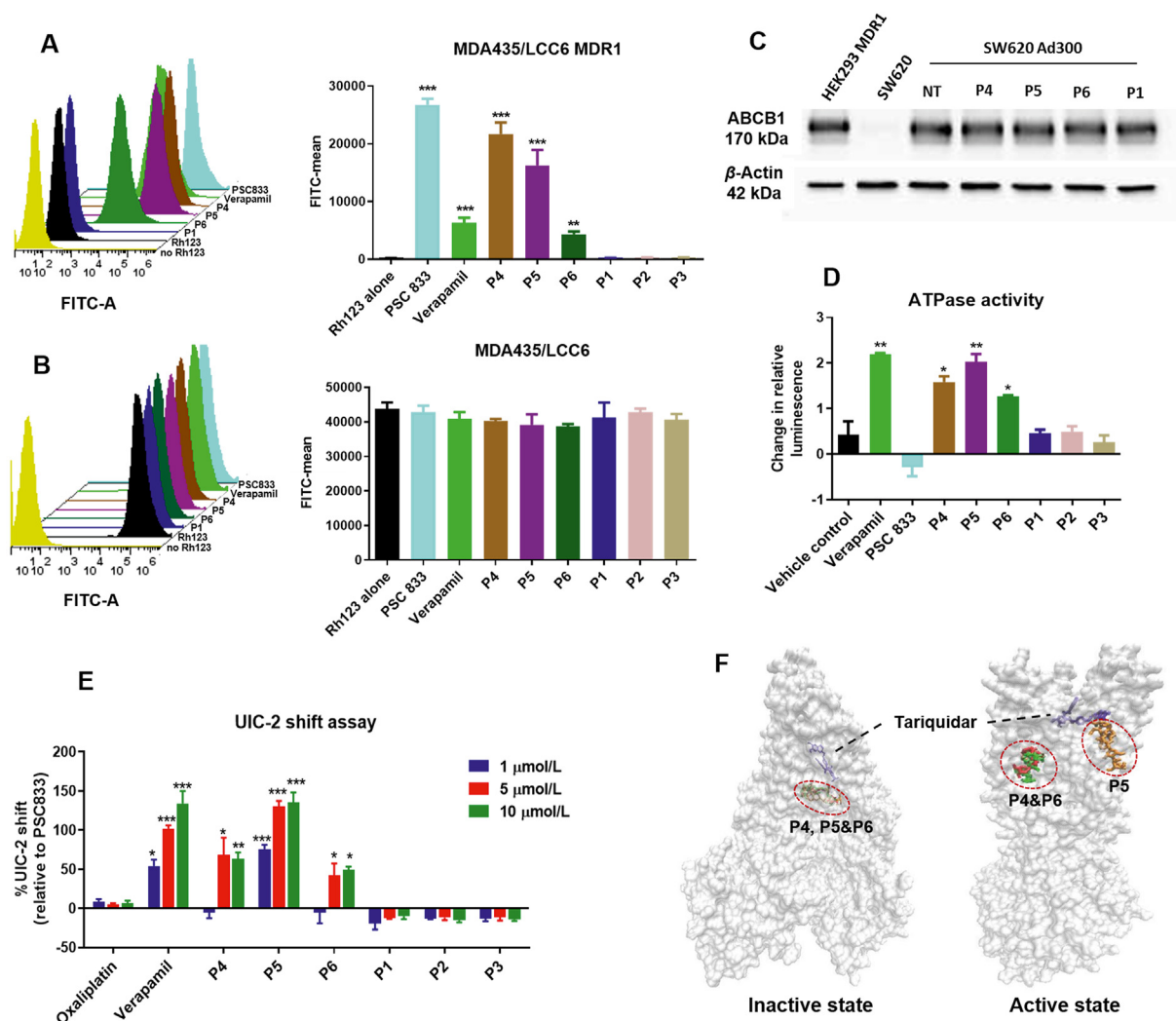


Figure 4 Mechanisms of ABCB1 inhibition by type II POPs. Representative flow cytometry histogram and fluorescence retention in MDA435/LCC6 MDR1 (A) and MDA435/LCC6 (B) cells incubated with ABCB1 substrate Rh123 in the absence or presence of individual POPs or positive controls (verapamil and PSC833) for 30 min plus a 1-h substrate-free efflux. $**P < 0.01$, $***P < 0.001$, compared to Rh123 alone group, by one-way ANOVA test followed by Tukey *post hoc* test. (C) Protein expression of ABCB1 in SW620 Ad300 cells treated with individual POPs. (D) Effects of individual POPs, verapamil, and PSC833 on ATPase activity of human recombinant ABCB1. $*P < 0.05$, $**P < 0.01$, $***P < 0.001$, compared to vehicle control, by one-way ANOVA test followed by Tukey *post hoc* test. (E) Relative shift of the mouse monoclonal ABCB1 antibody (UIC-2) in MDA435/LCC6 MDR1 cells treated with individual POPs. The results are presented as % UIC-2 shift (relative to IgG2b fluorescence signal) normalized to the signal of PSC833 (set as 100%). $*P < 0.05$, $**P < 0.01$, $***P < 0.001$, compared to oxaliplatin group, by two-way ANOVA test followed by Tukey *post hoc* test. (F) Molecular docking of type II POPs (P4, P5, and P6) to both inactive and active state of human ABCB1. Tariquidar, an ABCB1 inhibitor known to activate ABCB1, was also docked for a comparison. All data are expressed as mean \pm SD ($n = 3$). FITC, fluorescein isothiocyanate.

Table 3 Efflux ratio of type II POPs in Caco-2 cell monolayer.

Drug	P_{app} (10^{-6} cm/s)		Efflux ratio ^a
	A to B	B to A	
P4	1.52 \pm 0.16	1.53 \pm 0.16	1.010
P5	7.66 \pm 0.25	10.70 \pm 0.76	1.396
P6	6.38 \pm 0.52	9.12 \pm 0.86	1.429

^aEfflux ratio = P_{app} (B to A)/ P_{app} (A to B), where P_{app} (B to A) is the average of the permeability coefficient from basolateral to apical side; P_{app} (A to B) is the average of the permeability coefficient from apical to basolateral side.

combination treatment group, 4.2 ± 0.3 vs. 3.9 ± 1.4 h, $P > 0.05$) (Fig. 7C). Moreover, at 24 h after last paclitaxel dosing, tissue-to-plasma concentration ratios of paclitaxel in major organs (liver, lung, heart, spleen, and kidney) also showed no significant difference ($P > 0.05$) between two groups (Fig. 7D), suggesting the unchanged distribution profile. In addition, no brain accumulation of paclitaxel (Fig. 7E) and no abnormality in behavior and no significant weight losses of rats (Fig. 7F) in both treated groups were observed. The results indicate that type I POPs mixture in combination with paclitaxel has predictable pharmacokinetic interactions, in particular the significantly increased systemic exposure of paclitaxel, which provides a beneficial basis for the combination therapy for reversal of ABCB1-mediated MDR.

Table 4 Lowest binding energy (LBE) values of **P4**, **P5**, **P6**, and tariquidar docked to inactive or active conformation of human ABCB1 and the interacting amino acid residues at the drug-binding domain of human ABCB1.

Docking	LBE (kcal/mol)	Interacting amino acid residue ^a
ABCB1 (inactive conformation) ^b		
P4	-8.28 ± 0.33	Ala229, Ala230 , Trp232, Ala233, Lys234, Leu236, Ala295, Ser298 , Phe343, Gly346, and Gln990
P5	-8.27 ± 0.65	Ala229, Trp232, Ala233, Lys234 , Leu236, Ala295, Ser298 , Ile299, Gln347, and Pro350
P6	-8.35 ± 0.46	Ala229, Ala230 , Trp232, Ala233, Lys234 , Leu236, Ala295, Ser298 , Ile299, Ala302, Phe343, and Gln990
Tariquidar	-10.92 ± 0.56	Leu65, Met68, Met69, Phe72, Tyr310, Phe336, Leu339, Ile340, Phe343, Gln347, and Phe978
ABCB1 (active conformation)		
P4	-6.52 ± 0.25*	Ile840, Leu843, Ile847, Val865, Ile868, Ala869, Gly872, Thr941, Thr945, Val988, Val991, and Ser992
P5	-7.19 ± 0.38*	Val713, Phe716, Cys717, Ile720, Asn721, Leu724, Ala727, Leu758, Leu762, Ile765, Ser766, Thr769, and Leu772
P6	-6.80 ± 0.38*	Ile840, Leu843, Val865, Ile868, Ala869, Gly872, Val991, Ser992, Phe994, and Ala995
Tariquidar	-11.56 ± 1.35	Met69, Phe72, Leu332, Phe336, Leu339, Phe728, Ile731, Phe732, Ser733, Ile735, Ile736, Phe755, Leu758, Phe759, Leu762, Leu976, and Ser979

Data are presented as mean ± SD ($n = 3$). * $P < 0.05$, compared to the LBE value in docking to inactive-conformation ABCB1 by unpaired student's *t*-test.

^aAmino acid residues labeled in bold are forming hydrogen bond with the ligand.

^bData showing the docking to inactive-conformation of ABCB1 are retrieved from our previous study²⁴.

3.5. Oral administration of type I POPs did not cause toxicity in rats

After repeated daily oral doses of type I POPs mixture for 7 consecutive days, the rats revealed no obvious abnormality in behaviors and no weight losses, compared to the control rats. H&E staining of major tissues, including heart, liver, spleen, kidney, lung, and small intestines, also confirmed that type I POPs did not cause any observable toxicity in the treated rats (Fig. 8).

3.6. Type I POPs as ABCB1 modulating pro-drugs reversed ABCB1-mediated MDR of paclitaxel in LCC6 MDR1 tumor bearing mice

In MDA435/LCC6 breast tumor-bearing mice, the combination treatment of type I POPs mixture and paclitaxel showed no enhanced inhibitory effect on tumor growth caused by paclitaxel alone (Fig. 9A). However, in combination treatment, type I POPs mixture significantly potentiated antitumor effect of paclitaxel on drug-resistant MDA435/LCC6 MDR1 tumors (Fig. 9B), demonstrating that oral type I POPs circumvented the MDR of paclitaxel to ABCB1-overexpressing tumors in mice.

The results also revealed the comparable paclitaxel concentration increase in MDA435/LCC6 tumors (1.5 folds) and other organs (*i.e.*, heart, liver, kidney, and spleen) (1.4–2.1 folds) in the combination therapy group compared to that in paclitaxel alone group (Fig. 9C), suggesting that the increased paclitaxel concentration in MDA435/LCC6 tumors was due to the elevated systemic exposure of paclitaxel. On the other hand, in MDA435/LCC6 MDR1 tumors, the concentration of paclitaxel in combination therapy group was increased remarkably by 5.4 folds compared to that in paclitaxel alone group, while about 1.8–2.3 folds increases in other organs were observed in combination treatment group (Fig. 9D). The results demonstrate that combination therapy significantly enhances the penetration of paclitaxel into ABCB1-overexpressing MDA435/LCC6 MDR1 tumors due to the

significantly inhibited activity of overexpressed ABCB1 in tumors by bioactive POPs, and thereby overcome the ABCB1-mediated paclitaxel resistance.

4. Discussion

The presence of pro-drugs in natural products has long been recognized, while it is largely an unexplored area of research. Many pro-drugs devoid of direct pharmacological effects are usually excluded from further drug development. In the present study, we applied a sequential pharmacokinetics–pharmacodynamics study and for the first time demonstrated the ABCB1-specific modulatory effect of type I POPs (**P1**, **P2**, and **P3**) as natural pro-drugs derived from *M. tenacissima* and evaluated their applicability of reversing cancer MDR both *in vitro* and *in vivo*. Intriguingly, type II POPs (**P4**, **P5**, and **P6**), as the active metabolites of type I POPs, were only found in *M. tenacissima* at very low abundance (<0.01%, g/g), but can be readily bio-transformed in the body from type I POPs, the major ingredients (~50%, g/g) in *M. tenacissima*. Our study also represented as an example to identify new pro-drugs of MDR-reversal agents and to elucidate scientific basis of a clinically-used well-tolerated herbal medicine with previously unknown mechanisms of action.

Although more and more endeavors are advocated to discover novel ABCB1 modulators that are capable of inhibiting ABCB1-mediated drug efflux in MDR cancer cells, no ABCB1 inhibitor reported to date was able to prolong overall survival of cancer patients bearing MDR tumors⁴. The major limitation of the early developed agents, such as verapamil, cyclosporine A, and PSC833, is that they are usually not specific inhibitors of ABCB1. At MDR-reversing concentrations, they also lead to unacceptable toxicity⁸. Another critical issue is the unfavorable pharmacokinetic interaction⁸. Some ABCB1 modulators alter the activity of CYPs. Upon repeated dosing, they may also result in altered expression of ABCB1 and/or CYPs^{35–38}. Since many anticancer

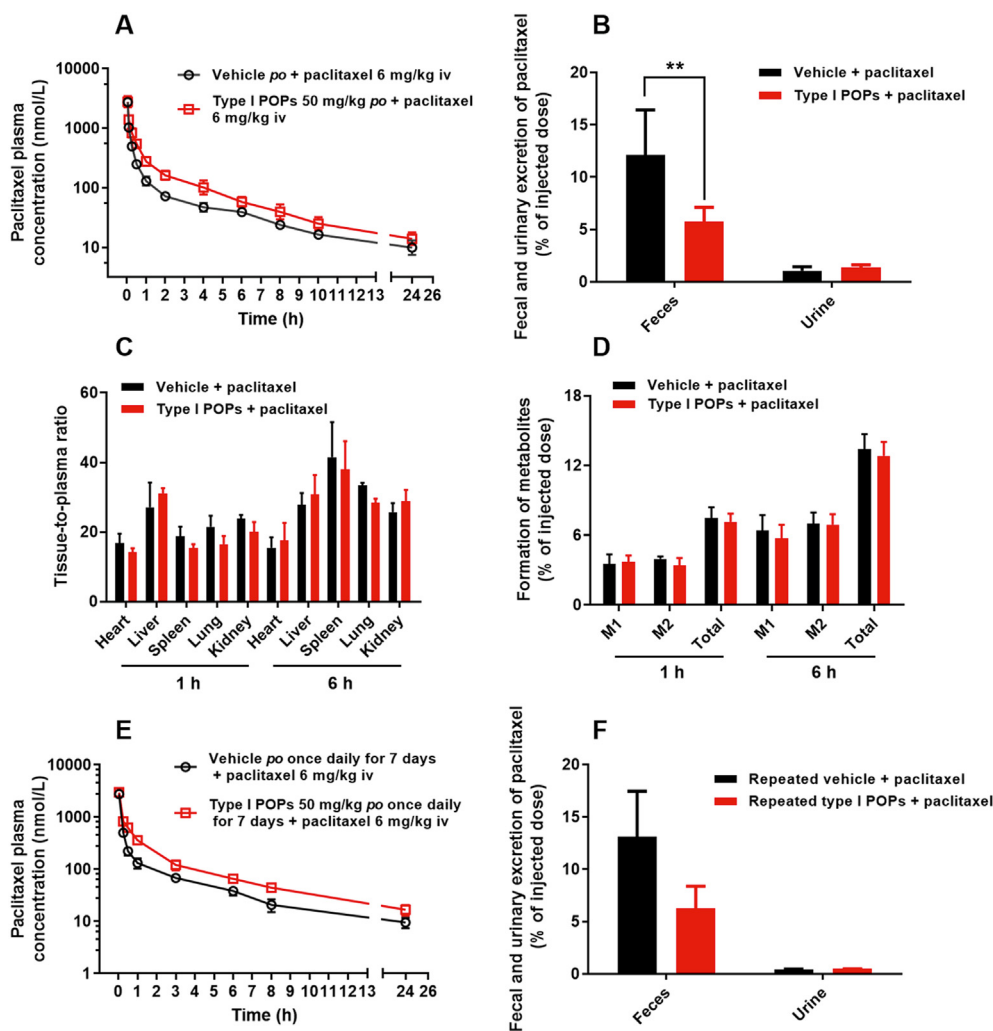


Figure 5 Effect of single or repeated oral doses of type I POPs mixture on pharmacokinetics of paclitaxel in rats. Plasma concentration vs. time profiles (A), fecal and urinary excretion within 0–24 h (B), tissue distribution profile (C), and metabolism (D) of paclitaxel (6 mg/kg) intravenously injected after a single oral dose of vehicle or type I POPs (50 mg/kg). Metabolism of paclitaxel was monitored by the total amount of its two major metabolites, M1 (*p*-3'-hydroxylpaclitaxel) and M2 (*m*-2'-hydroxylpaclitaxel) in bile, tissues and plasma at 1 and 6 h post paclitaxel administration. Plasma concentration vs. time profiles (E) and fecal and urinary excretion within 0–24 h (F) of paclitaxel (6 mg/kg) intravenously injected after a 7-day repeated oral dose of vehicle or type I POPs (50 mg/kg). All data are expressed as mean \pm SD ($n = 6$). ** $P < 0.01$, by Student's *t*-test.

drugs are both substrates of ABCB1 and CYPs, the aforementioned factors often lead to unpredictable pharmacokinetic interactions, thus making it difficult to establish a safe but effective dosage regimen of combination of ABCB1 modulators and anti-cancer drugs³⁹. Therefore, ideal ABCB1 modulators should be specific and non-toxic, and produce no or predictable pharmacokinetic interactions. In the present study, one of the main findings is that type II POPs show advantages over other ABCB1 inhibitors reported in the literature. We firstly demonstrated that type II POPs significantly abrogated ABCB1-mediated chemoresistance in MDR cells. Further mechanistic studies suggested that, unlike verapamil (a substrate and competitive inhibitor of ABCB1) and PSC833 (a non-competitive inhibitor of ABCB1), type II POPs were not ABCB1 substrates, did not affect ABCB1 expression, and served as non-competitive inhibitors of ABCB1 *via* altering ABCB1 into a conformation that increased the binding of UIC-2 and stimulated ATPase activity. Docking studies showed that type II POPs were well fitted into the drug cavity of human

ABCB1 and displayed multiple drug binding sites which differ from verapamil and PSC833 but share similarity to tariquidar. Taken together, the advantages of using these POPs as ABCB1 inhibitors include: (1) type II POPs were effective in reversing MDR *in vitro* at concentrations above 0.4 $\mu\text{mol/L}$ ²⁴. Their effects were 2.5–4.6 times superior to or at least comparable to that of verapamil; (2) type II POPs were devoid of cytotoxicity at MDR-reversing concentrations (Supporting Information Fig. S4); (3) type II POPs were much more selective toward ABCB1 compared to the other two major efflux transporters, ATP binding cassette subfamily C member 1 (ABCC1), and ATP binding cassette subfamily G member 2 (ABCG2)²⁴; and (4) type II POPs were not the competitive inhibitors of ABCB1. Therefore, type II POPs were safe, potent and specific ABCB1 inhibitors, which displayed a unique mechanism of action (Table 7^{7,11,24,39–43}).

Moreover, type I POPs were identified as pro-drugs with druggable characteristics. We showed that type I POPs (P1, P2, and P3) were significantly biotransformed to type II POPs (P4,

Table 5 Pharmacokinetic parameters of paclitaxel after single or repeated oral doses of type I POPs mixture to rats.

Parameter	Vehicle	Type I	Repeated Vehicle	Repeated type
	A + paclitaxel	POP + paclitaxel	A + paclitaxel	I POP + paclitaxel
$t_{1/2}$ (h)	3.2 ± 0.7	3.0 ± 0.3	2.8 ± 0.8	2.7 ± 0.7
C_{max} (nmol/L)	2769 ± 197	2830 ± 640	2795 ± 17	2991 ± 143
AUC _{0-∞} (nmol·h/L)	1278 ± 28	1969 ± 257**	1285 ± 180	2241 ± 223***
AUC _{0-24 h} (nmol·h/L)	1149 ± 68	1860 ± 270**	1240 ± 188	2040 ± 277***
CL (L/h/kg)	5.5 ± 0.1	3.6 ± 0.5***	5.5 ± 0.7	3.3 ± 0.3***
V_d (L/kg)	31.5 ± 7.5	16.0 ± 2.3**	29.2 ± 1.6	13.09 ± 4.63**
MRT _{0-24 h} (h)	5.3 ± 1.0	4.5 ± 0.6	4.6 ± 1.6	4.9 ± 1.6

** $P < 0.01$, *** $P < 0.001$, compared to the corresponding vehicle + paclitaxel group. Data are presented as mean ± SD ($n = 6$).

Table 6 Effect of individual POPs on the activity of major cytochrome P450 isozymes in rat liver microsomes determined by cocktail assay.

CYP isozyme (probe substrate)	Metabolite formation (%) of individual probe substrate with/without individual POP (10 μmol/L, $n = 3$)							
	Negative control ^a	Blank ^b	P1	P2	P3	P4	P5	P6
CYP3A (nifedipine)	N.D.	39.5 ± 2.7	43.2 ± 3.4	41.0 ± 2.8	43.5 ± 3.8	43.7 ± 1.2	38.2 ± 1.4	37.3 ± 1.4
CYP2C11 (<i>S</i> -mephenytoin)	N.D.	16.8 ± 0.9	18.2 ± 0.7	17.1 ± 1.0	17.6 ± 0.9	17.3 ± 0.7	16.9 ± 1.2	17.2 ± 0.9
CYP2A1 (coumarin)	N.D.	61.4 ± 1.6	61.1 ± 2.6	61.0 ± 1.1	62.1 ± 1.6	62.1 ± 1.1	60.9 ± 2.6	60.8 ± 0.5
CYP2B1 (bupropion)	N.D.	25.5 ± 1.6	22.2 ± 2.4	29.3 ± 1.8	25.1 ± 5.7	22.5 ± 1.6	21.9 ± 2.0	22.7 ± 0.2
CYP2D1 (dextromethorphan)	N.D.	31.1 ± 3.8	29.7 ± 2.5	27.2 ± 1.4	30.7 ± 0.8	30.2 ± 1.9	31.5 ± 3.1	28.3 ± 2.6
CYP1A2 (phenacetin)	N.D.	20.7 ± 1.0	20.3 ± 2.2	22.4 ± 0.5	20.9 ± 2.0	19.6 ± 2.4	20.3 ± 1.1	19.4 ± 1.8

^aNegative control: denatured rat liver microsomes were used.

^bBlank: incubation system in the absence of POPs.

P5, and **P6**) both *in vitro* and *in vivo*. Notably, the biotransformation rate was nearly 100%, which might be due to the fact that a readily-found enzyme in almost all intestinal microbiota, β -glucosidase, was responsible for the bioconversion. We also demonstrated that oral administration of type I POPs at 50 mg/kg/day was adequate to maintain the concentrations of type II POPs *in vivo* above 0.4 μmol/L (the MDR-reversing concentration *in vitro*) for 4–8 h (Fig. 2A). Thus, type I POPs as prodrugs can be potentially used for overcoming ABCB1-mediated chemoresistance *in vivo*.

Furthermore, we demonstrated that the ABCB1 inhibitory prodrugs type I POPs were safe *in vivo*, and induced predictable pharmacokinetic interaction with no obvious toxicity. We further showed that single and daily repeated doses of type I POPs elevated systemic exposure of paclitaxel to the similar extent. Despite the change of systemic exposure, it should be noted that major pharmacokinetic parameters such as C_{max} , MRT_{0-∞}, and $t_{1/2}$ were not altered, which may presumably be explained by the following findings: (1) oral administration of type I POPs did not significantly change the distribution profile and metabolism of paclitaxel; (2) the active metabolites of type I POPs, namely **P4**, **P5**, and **P6**, did not affect the activity of major hepatic CYPs; and (3) repeated doses of type I POPs did not alter the expression of CYPs and ABCB1 in the body. These characteristics have largely distinguished the POPs from most previously developed ABCB1 modulators, which often induced CYPs and ABCB1 interplay, and caused complicated pharmacokinetic interaction by altering the expression of CYPs and/or ABCB1 after repeated doses^{36,44}. In contrast, repeated dosing of the combination therapy (type I POPs mixture plus paclitaxel) produced a repeatable pharmacokinetic interaction, which was characterized by no significant systemic

accumulation, unchanged tissue distribution profile and unchanged elimination $t_{1/2}$ value. The combination treatment also did not show appreciable toxicity (no brain accumulation and no body weight loss) *in vivo*.

The MDR reversal effect of type I POPs was also demonstrated *in vivo* in drug-resistant and ABCB1-overexpressing MDA435/LCC6 MDR1 tumor-bearing mice. Oral administration of type I POPs mixture overcame ABCB1-mediated MDR of paclitaxel by increasing the intratumoral penetration of paclitaxel. While, the distribution profiles of paclitaxel in other tissues were not remarkably affected. The MDR-reversal effect was specific, because type I POPs did not affect the antitumor activity of paclitaxel in sensitive MDA435/LCC6 tumor-bearing mice.

Consequently, our findings added significant knowledge to understand the combinational use of Xiao-ai-ping, a standardized herbal extract of *M. tenacissima*, via oral ingestion with chemotherapeutics. As an herb-derived anticancer prescription drug, Xiao-ai-ping has both oral and injectable formulations. Previous studies have suggested that the oral or injectable Xiao-ai-ping was effective in combinational chemotherapies against several cancer types^{45,46}. Based on the current and previous investigations on the chemical basis and underlying mechanisms of Xiao-ai-ping, its anticancer actions included multiple modes. Firstly, Xiao-ai-ping alone (particularly via injection route) exhibits direct anticancer effect in different cancer cell lines and animal tumor xenografts^{47,48}. Secondly, the injectable Xiao-ai-ping enhances the antitumor effects of several anticancer drugs through various mechanisms including the inhibition of CYP3A4 activity, down-regulation of activating transcription factor 3 (ATF3), and suppression of pregnane X receptor (PXR) expression and downstream targets^{49–51}. Moreover, our research team also

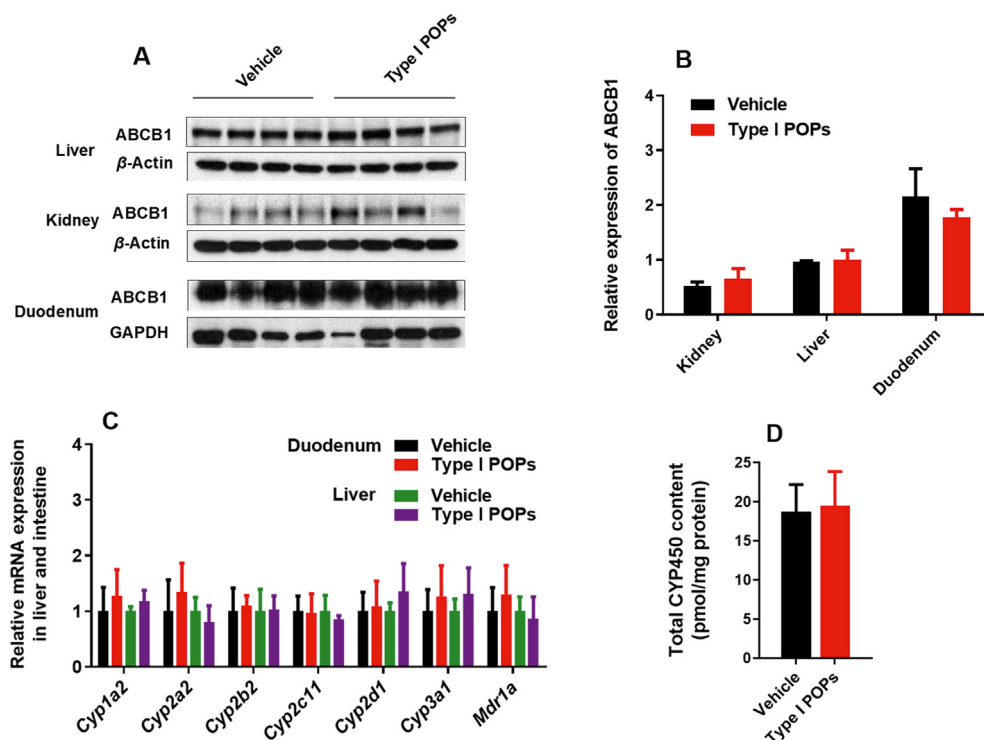


Figure 6 Effect of repeated oral doses of type I POPs mixture on the expression of ABCB1 and CYPs in rats ($n = 4$) treated with type I POPs at 50 mg/kg per day for 7 consecutive days. ABCB1 expression in rat liver, kidney, and duodenum tissues evaluated by Western blot (loading control: β -actin or GAPDH) (A). Relative Western blot signals were quantified by Image J after normalization to β -actin or GAPDH (B). Quantitative PCR analysis of gene expression of major CYPs and *ABCB1* (*Mdr1a*) performed in rat liver and intestine tissues (C). Total cytochrome P450 (CYP450) content measured in liver microsomes prepared from the treated rats (D). All data are expressed as mean \pm SD ($n = 4$).

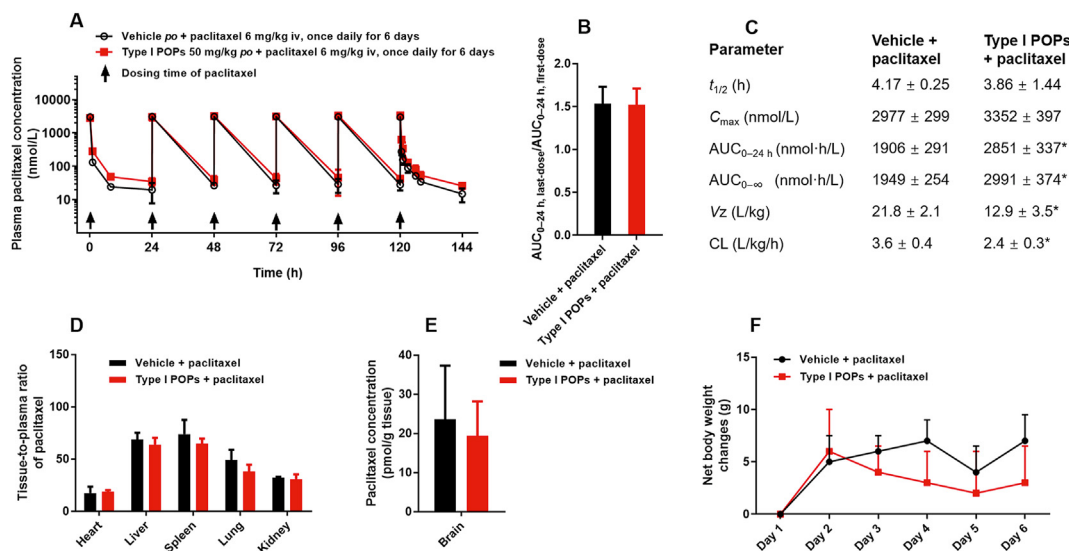


Figure 7 Effects of type I POPs mixture (*po*, 50 mg/kg/day for 6 consecutive days) on pharmacokinetics, distribution, and safety of repeatedly dosed paclitaxel (*iv*, 6 mg/kg/day for 6 consecutive days) in rats. Plasma concentration vs. time profiles of paclitaxel (A), $AUC_{0-24 h, last-dose}/AUC_{0-24 h, first-dose}$ ratio of paclitaxel (B), pharmacokinetic parameters of the last-dose of paclitaxel (C), distribution profile (tissue-to-plasma concentration ratio) of paclitaxel (D) and brain accumulation of paclitaxel (E) in rats at 24 h after the last-dose paclitaxel, and the net body weight changes of rats (F). All data are expressed as mean \pm SD ($n = 6$). * $P < 0.05$, compared to vehicle + paclitaxel group, by Student's *t*-test.

reported that several POPs in *M. tenacissima* inhibited the MDR ABC transporters and potentiated the cytotoxic effect of chemotherapeutic drugs previously²⁴. However, to date, there is no

evidence demonstrating the anticancer effect of *M. tenacissima* and Xiao-ai-ping through oral route. Therefore, the present study is the first report to demonstrate the major constituents of *M.*

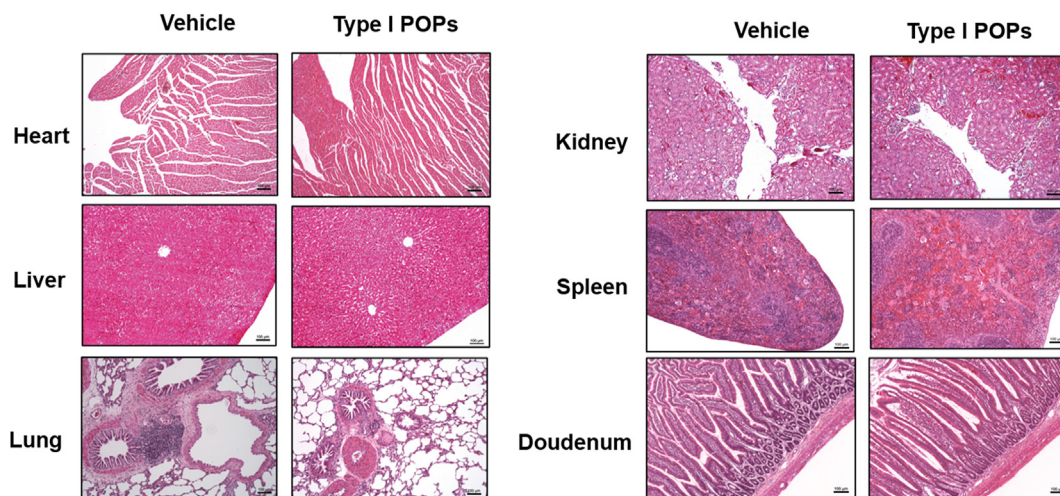


Figure 8 Effect of repeated oral doses of type I POPs mixture (50 mg/kg/day for 7 consecutive days) on safety of rats. Hematoxylin and eosin (H&E) staining of major tissues, including heart, liver, lung, kidney, spleen, and duodenum in the treated rats was viewed under microscope using 10 × magnification. Scale bar = 100 μm.

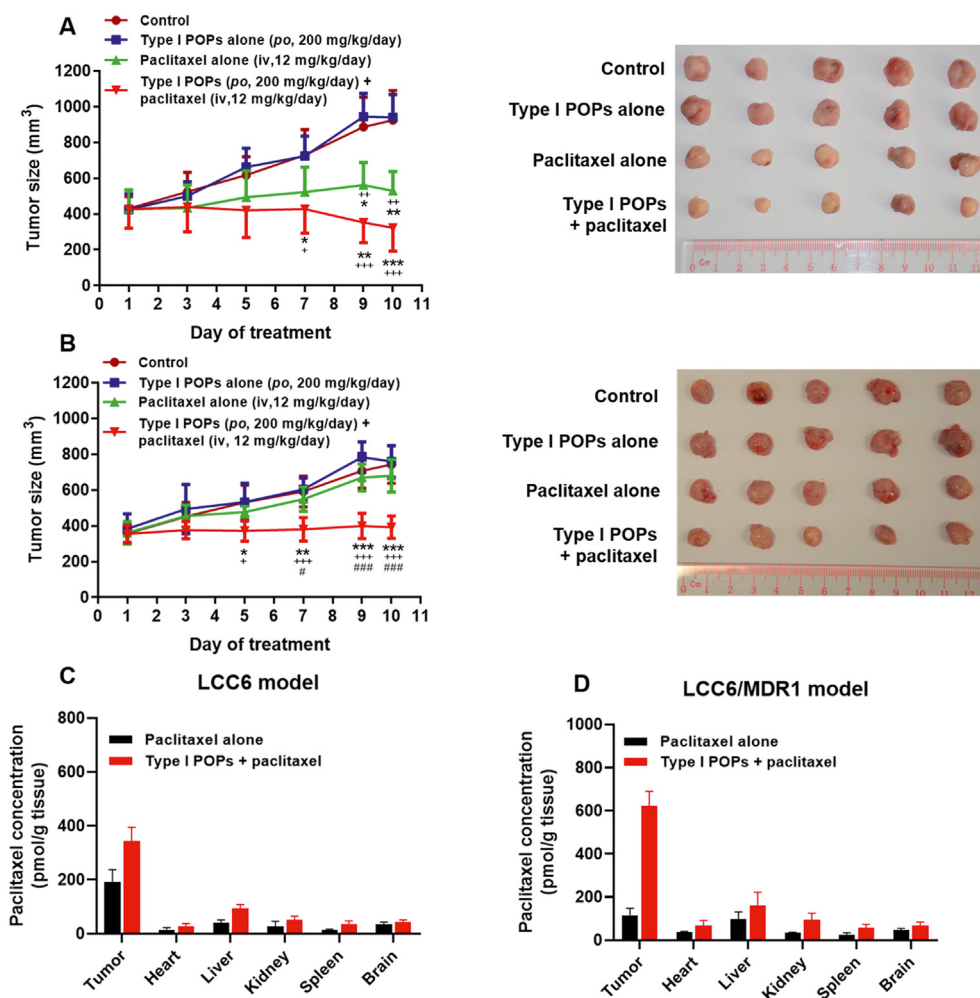


Figure 9 Anti-cancer effect of paclitaxel, type I POPs mixture, and their combination in MDA435/LCC6 (A) and MDA435/LCC6 MDR1 (B) tumor-bearing mice. Tumor and tissue distribution of paclitaxel in MDA435/LCC6 (C) and MDA435/LCC6 MDR1 (D) tumor-bearing mice after sacrifice. Data are expressed as mean ± SD ($n = 5$). * $P < 0.05$, ** $P < 0.01$, *** $P < 0.001$, compared to control group; # $P < 0.05$, ### $P < 0.001$, compared to paclitaxel alone group; + $P < 0.05$, ++ $P < 0.01$, +++ $P < 0.001$, compared to type I POPs alone group, by two-way ANOVA followed by Tukey *post hoc* test.

Table 7 Comparison of type II POPs with known ABCB1 inhibitors.

Comparison	Type II POP	Verapamil	PSC833	Tariquidar
Inhibitory potency	++	+	+++	+++ ⁴⁰
Selectivity ^{7,41}	++	×	+++	+++
Pharmacokinetics interaction:				
Affect CYPs activity ^{7,39}	×	√	√	×
Induce drug–drug interaction	+	+++ ¹¹	+++ ¹¹	× ⁷
Mechanism:				
ABCB1 substrate	×	√	×	×
Alter ABCB1 expression	×	√ ⁴²	√ ⁴³	N.A.
Activate ATPase	√	√	×	× ⁴⁰
Binding site	Binding to drug cavity in a way similar to tariquidar, but with alternative binding sites	Both binding with different sites from type II POPs ²⁴		Binding to drug cavity at different site from type II POPs

×, no or negative; √, yes or positive; +, low; ++, moderate; +++, high.

tenacissima, type I POPs, as prodrugs after oral administration to reverse chemotherapeutic MDR *via* modulating ABCB1. Our interesting findings would facilitate new drug development from *M. tenacissima* and potentially support its use through oral ingestion in combination with other anticancer drugs.

5. Conclusions

Type I POPs (**P1**, **P2**, and **P3**) isolated from *M. tenacissima* were identified as novel ABCB1-modulating pro-drugs that have been demonstrated to be safe, potent, and specific, and are promising to be further developed for circumventing ABCB1-mediated MDR in clinic. Since **P1**, **P2**, and **P3** are the major constituents of *M. tenacissima* extract, the sole herb extract of the NMPA-approved proprietary herbal medicine Xiao-ai-ping, this study for the first time provided scientific data for the use of Xiao-ai-ping (particularly through oral ingestion) and its major constituents in combination chemotherapy. In addition, the strategy to identify active constituents from herbal preparations with long-time clinical uses to overcome the resistance of other conventional drugs may be a promising direction in the field of adjuvant chemotherapy.

Acknowledgments

We thank Dr. Susan E. Bates (NCI, NIH, Bethesda, MD, USA) and Dr. Robert Clarke (Georgetown University, Washington DC, USA) for providing the sensitive and resistant cancer cell lines. This work was supported by Health and Medical Research Fund (HHSRF Project No. 08090481, Hong Kong SAR, China) from Food and Health Bureau, HKSAR, One-off Funding for Joint Lab/Research collaboration (Project code: 3132968, Hong Kong SAR, China) from the Chinese University of Hong Kong and Seed Fund for Joint Establishments from School of Biomedical Science, the Chinese University of Hong Kong (China).

Author contributions

Xu Wu, Chun Yin, and Jiang Ma conceived the project, contributed to the experimental designs, performed experiments, interpreted the results, generated figures, and wrote the manuscript; Kenneth Kin-Wah To and Ge Lin conceived and supervised the

project, interpreted the results and wrote the manuscript; Sheng Yao and Yang Ye provided the isolated POPs from *M. tenacissima*; Onat Kadioglu and Thomas Efferth performed docking analysis; Stella Chai and Chunyuan Zhang performed parts of the experiments. All authors discussed the results and revision of the manuscript, and approved the manuscript.

Conflicts of interest

Yang Ye, Ge Lin, Kenneth Kin-Wah To, Sheng Yao, and Chun Yin have a patent granted in China (No. CN201380031642.1) related to this work. Other authors have declared no potential conflicts of interest.

Appendix A. Supporting information

Supporting data to this article can be found online at <https://doi.org/10.1016/j.apsb.2020.12.021>.

References

- Aller SG, Yu J, Ward A, Weng Y, Chittaboina S, Zhuo R, et al. Structure of P-glycoprotein reveals a molecular basis for poly-specific drug binding. *Science* 2009;**323**:1718–22.
- Juliano RL, Ling V. A surface glycoprotein modulating drug permeability in Chinese hamster ovary cell mutants. *Biochim Biophys Acta* 1976;**455**:152–62.
- Van der Blik AM, Van der Velde-Koerts T, Ling V, Borst P. Overexpression and amplification of five genes in a multidrug-resistant Chinese hamster ovary cell line. *Mol Cell Biol* 1986;**6**:1671–8.
- Binkhathlan Z, Lavasanifar A. P-glycoprotein inhibition as a therapeutic approach for overcoming multidrug resistance in cancer: current status and future perspectives. *Curr Cancer Drug Targets* 2013;**13**:326–46.
- Coley HM. Overcoming multidrug resistance in cancer: clinical studies of P-glycoprotein inhibitors. *Multi-Drug Resist Cancer* 2010;**596**:341–58.
- Darby RAJ, Callaghan R, McMahon RM. P-glycoprotein inhibition: the past, the present and the future. *Curr Drug Metabol* 2011;**12**:722–31.
- Fox E, Widemann BC, Pastakia D, Chen CC, Yang SX, Cole D, et al. Pharmacokinetic and pharmacodynamic study of tariquidar (XR9576), a P-glycoprotein inhibitor, in combination with doxorubicin,

- vinorelbine, or docetaxel in children and adolescents with refractory solid tumors. *Cancer Chemother Pharmacol* 2015;**76**:1273–83.
8. Thomas H, Coley HM. Overcoming multidrug resistance in cancer: an update on the clinical strategy of inhibiting p-glycoprotein. *Can Contract* 2003;**10**:159–65.
 9. Wang YJ, Zhang YK, Zhang GN, Rihani SB, Wei MN, Gupta P, et al. Regorafenib overcomes chemotherapeutic multidrug resistance mediated by ABCB1 transporter in colorectal cancer: *in vitro* and *in vivo* study. *Cancer Lett* 2017;**396**:145–54.
 10. Hsiao SH, Murakami M, Yeh N, Li YQ, Hung TH, Wu YS, et al. The positive inotropic agent DPI-201106 selectively reverses ABCB1-mediated multidrug resistance in cancer cell lines. *Cancer Lett* 2018;**434**:81–90.
 11. Shukla S, Wu CP, Ambudkar SV. Development of inhibitors of ATP-binding cassette drug transporters: present status and challenges. *Expert Opin Drug Metabol Toxicol* 2008;**4**:205–23.
 12. Pajeva IK, Sterz K, Christlieb M, Steggemann K, Marighetti F, Wiese M. Interactions of the multidrug resistance modulators tariquidar and elacridar and their analogues with P-glycoprotein. *ChemMedChem* 2013;**8**:1701–13.
 13. Han SY, Zhao MB, Zhuang GB, Li PP. *Marsdenia tenacissima* extract restored gefitinib sensitivity in resistant non-small cell lung cancer cells. *Lung Cancer* 2012;**75**:30–7.
 14. Huang ZR, Wang Y, Chen JJ, Wang RP, Chen Q. Effect of Xiaoaiping injection on advanced hepatocellular carcinoma in patients. *J Tradit Chin Med* 2013;**33**:34–8.
 15. Xia G. Effect of xiaoaiping injection combined with TP regimen in the treatment of advanced non-small cell lung cancer. *Proc Clin Med* 2013;**22**:83–5.
 16. Zhu RJ, Shen XL, Dai LL, Ai XY, Tian RH, Tang R, et al. Total aglycones from *Marsdenia tenacissima* increases antitumor efficacy of paclitaxel in nude mice. *Molecules* 2014;**19**:13965–75.
 17. Sun Y, Zhao Z. Clinical study on cancer-eliminating injection by intervention therapy through hepatic artery in metastatic liver cancer Shanghai. *J Tradit Chin Med* 2000;**34**:14–7.
 18. Wang W, Zhou Y, Zhang X, Gao T, Luo Z, Liu M. A random study of xiaoaiping injection combined with chemotherapy on the treatment of advanced non-small cell lung cancer. *Chin Clin Oncol* 2009;**14**:936–8.
 19. Huang Z, Tan H, Wang C, Zhang H, Liu D, Zhou C, et al. Clinical research of combined xiaoaiping injection with chemotherapy on advanced non-small cell lung cancer. *Chin Clin Oncol* 2007;**12**:97–9.
 20. Hu YJ, Shen XL, Lu HL, Zhang YH, Huang XA, Fu LC, et al. Tenacigenin B derivatives reverse P-glycoprotein-mediated multidrug resistance in HepG2/Dox cells. *J Nat Prod* 2008;**71**:1049–51.
 21. Yao S, To KK, Ma L, Yin C, Tang C, Chai S, et al. Polyoxypregnane steroids with an open-chain sugar moiety from *Marsdenia tenacissima* and their chemoresistance reversal activity. *Phytochemistry* 2016;**126**:47–58.
 22. Yao S, To KK, Wang YZ, Yin C, Tang C, Chai S, et al. Polyoxypregnane steroids from the stems of *Marsdenia tenacissima*. *J Nat Prod* 2014;**77**:2044–53.
 23. Wu X, Zhu L, Ma J, Ye Y, Lin G. Adduct ion-targeted qualitative and quantitative analysis of polyoxypregnanes by ultra-high pressure liquid chromatography coupled with triple quadrupole mass spectrometry. *J Pharmaceut Biomed Anal* 2017;**145**:127–36.
 24. To KKW, Wu X, Yin C, Chai S, Yao S, Kadioglu O, et al. Reversal of multidrug resistance by *Marsdenia tenacissima* and its main active ingredients polyoxypregnanes. *J Ethnopharmacol* 2017;**203**:110–9.
 25. Lai GM, Chen YN, Mickley LA, Fojo AT, Bates SE. P-glycoprotein expression and schedule dependence of adriamycin cytotoxicity in human colon carcinoma cell lines. *Int J Cancer* 1991;**49**:696–703.
 26. Li XQ, Wang L, Lei Y, Hu T, Zhang FL, Cho CH, et al. Reversal of P-gp and BCRP-mediated MDR by tariquidar derivatives. *Eur J Med Chem* 2015;**101**:560–72.
 27. Ruan JQ, Leong WI, Yan R, Wang YT. Characterization of metabolism and *in vitro* permeability study of notoginsenoside R1 from *Radix notoginseng*. *J Agric Food Chem* 2010;**58**:5770–6.
 28. Silva R, Carmo H, Dinisoliveira R, Cordeirodasilva A, Lima SC, Carvalho F, et al. *In vitro* study of P-glycoprotein induction as an antidotal pathway to prevent cytotoxicity in Caco-2 cells. *Arch Toxicol* 2011;**85**:315–26.
 29. Kadioglu O, Saeed MEM, Valoti M, Frosini M, Sgaragli G, Efferth T. Interactions of human P-glycoprotein transport substrates and inhibitors at the drug binding domain: functional and molecular docking analyses. *Biochem Pharmacol* 2016;**104**:42–51.
 30. Turpeinen M, Jouko U, Jorma J, Olavi P. Multiple P450 substrates in a single run: rapid and comprehensive *in vitro* interaction assay. *Eur J Pharmaceut Sci* 2005;**24**:123–32.
 31. Zhu L, Xue J, Xia Q, Fu PP, Lin G. The long persistence of pyrrolizidine alkaloid-derived DNA adducts *in vivo*: kinetic study following single and multiple exposures in male ICR mice. *Arch Toxicol* 2017;**91**:949–65.
 32. Omura T, Sato R. The carbon monoxide-binding pigment of liver microsomes. II. Solubilization, purification, and properties. *J Biol Chem* 1964;**239**:2379–85.
 33. Higgins CF. Multiple molecular mechanisms for multidrug resistance transporters. *Nature* 2007;**446**:749–57.
 34. Loo TW, Bartlett MC, Detty MR, Clarke DM. The ATPase activity of the P-glycoprotein drug pump is highly activated when the N-terminal and central regions of the nucleotide-binding domains are linked closely together. *J Biol Chem* 2012;**287**:26806.
 35. Kageyama M, Namiki H, Fukushima H, Ito Y, Shibata N, Takada K. *In vivo* effects of cyclosporin A and ketoconazole on the pharmacokinetics of representative substrates for P-glycoprotein and cytochrome P450 (CYP) 3A in rats. *Biol Pharm Bull* 2005;**28**:316–22.
 36. Lee CK, Ki SH, Choi JS. Effects of oral curcumin on the pharmacokinetics of intravenous and oral etoposide in rats: possible role of intestinal CYP3A and P-gp inhibition by curcumin. *Biopharm Drug Dispos* 2011;**32**:245–51.
 37. Rajnarayana K, Reddy MS, Vidyasagar J, Krishna DR. Study on the influence of silymarin pretreatment on metabolism and disposition of metronidazole. *Arzneimittelforschung* 2004;**54**:109–13.
 38. Zhang W, Tan TM, Lim LY. Impact of curcumin-induced changes in P-glycoprotein and CYP3A expression on the pharmacokinetics of peroral celirolol and midazolam in rats. *Drug Metab Dispos* 2007;**35**:110–5.
 39. Fischer V, Rodriguez-Gascon A, Heitz F, Tynes R, Hauck C, Cohen D, et al. The multidrug resistance modulator valsopodar (PSC 833) is metabolized by human cytochrome P450 3A — implications for drug-drug interactions and pharmacological activity of the main metabolite. *Drug Metab Dispos* 1998;**26**:802–11.
 40. Fox E, Bates SE. Tariquidar (XR9576): a P-glycoprotein drug efflux pump inhibitor. *Expert Rev Anticancer Ther* 2007;**7**:447–59.
 41. Kannan P, Telu S, Shukla S, Ambudkar SV, Pike VW, Halldin C, et al. The “specific” P-glycoprotein inhibitor tariquidar is also a substrate and an inhibitor for breast cancer resistance protein (BCRP/ABCG2). *ACS Chem Neurosci* 2011;**2**:82–9.
 42. Muller C, Bailly JD, Goubin F, Laredo J, Jaffrézou JP, Bordier C, et al. Verapamil decreases P-glycoprotein expression in multidrug-resistant human leukemic cell lines. *Int J Cancer* 1994;**56**:749–54.
 43. Bark H, Choi CH. PSC833, cyclosporine analogue, downregulates MDR1 expression by activating JNK/c-Jun/AP-1 and suppressing NF-kappaB. *Cancer Chemother Pharmacol* 2010;**65**:1131–6.
 44. Lim SC, Choi JS. Effects of naringin on the pharmacokinetics of intravenous paclitaxel in rats. *Biopharm Drug Dispos* 2006;**27**:443–7.
 45. Feng F, Huang J, Wang Z, Zhang J, Han D, Wu Q, et al. Xiao-ai-ping injection adjunct with platinum-based chemotherapy for advanced non-small-cell lung cancer: a systematic review and meta-analysis. *BMC Complement Med Ther* 2020;**20**:3.
 46. Zhou X, Liu M, Ren Q, Zhu W, Wang Y, Chen H, et al. Oral and injectable *Marsdenia tenacissima* extract (MTE) as adjuvant therapy to chemotherapy for gastric cancer: a systematic review. *BMC Compl Alternative Med* 2019;**19**:366.
 47. Li D, Li C, Song Y, Zhou M, Sun X, Zhu X, et al. *Marsdenia tenacissima* extract and its functional components inhibits proliferation and induces apoptosis of human Burkitt leukemia/lymphoma cells *in vitro* and *in vivo*. *Leuk Lymphoma* 2016;**57**:419–28.

48. Ye B, Yang J, Li J, Niu T, Wang S. *In vitro* and *in vivo* antitumor activities of tenacissoside C from *Marsdenia tenacissima*. *Planta Med* 2014;**80**:29–38.
49. Chen J, Zhang X, Xiao X, Ding Y, Zhang W, Shi M, et al. Xiao-ai-ping injection enhances effect of paclitaxel to suppress breast cancer proliferation and metastasis *via* activating transcription factor 3. *Integr Cancer Ther* 2020;**19**. Available from: <https://doi.org/10.1177/1534735420906463>. 1534735420906463.
50. Zhang XQ, Ding YW, Chen JJ, Xiao X, Zhang W, Zhou L, et al. Xiaoaiping injection enhances paclitaxel efficacy in ovarian cancer *via* pregnane X receptor and its downstream molecules. *J Ethnopharmacol* 2020;**261**:113067.
51. Xie B, Lu YY, Luo ZH, Qu Z, Zheng CG, Huang XA, et al. Tenacigenin B ester derivatives from *Marsdenia tenacissima* actively inhibited CYP3A4 and enhanced *in vivo* antitumor activity of paclitaxel. *J Ethnopharmacol* 2019;**235**:309–19.